FFI RAPPORT

BOTTOM REVERBERATION PREDICTIONS WITH THE ACOUSTIC MODEL LYBIN: A Comparison between three Bottom Backscattering Algorithms

SEVALDSEN Erik

FFI/RAPPORT-2002/02367

FFIE/795/161.4

Approved
Kjeller 12. September 2002

John-Mikal Størdal
Director of Research

BOTTOM REVERBERATION PREDICTIONS WITH THE ACOUSTIC MODEL LYBIN:
A Comparison between three Bottom Backscattering Algorithms

SEVALDSEN Erik

FFI/RAPPORT-2002/02367

FORSVARETS FORSKNINGSINSTITUTT
Norwegian Defence Research Establishment
P O Box 25, NO-2027 Kjeller, Norway

FORSVARETS FORSKNINGSINSTITUTT (FFI)
Norwegian Defence Research Establishment

P O BOX 25
N0-2027 KJELLER, NORWAY

UNCLASSIFIED

SECURITY CLASSIFICATION OF THIS PAGE
(when data entered)

REPORT DOCUMENTATION PAGE

1) PUBL/REPORT NUMBER	2) SECURITY CLASSIFICATION	3) NUMBER OF PAGES
FFI/RAPPORT-2002/02367	UNCLASSIFIED	51
1a) PROJECT REFERENCE	2a) DECLASSIFICATION/DOWNGRADING SCHEDULE	
FFIE/795/161.4	-	

4) TITLE

BOTTOM REVERBERATION PREDICTIONS WITH THE ACOUSTIC MODEL LYBIN:
A Comparison between three Bottom Backscattering Algorithms

5) NAMES OF AUTHOR(S) IN FULL (surname first)

SEVALDSEN Erik

6) DISTRIBUTION STATEMENT

Approved for public release. Distribution unlimited. (Offentlig tilgjengelig)

7) INDEXING TERMS

	IN ENGLISH:		IN NORWEGIAN:
a)	Bottom backscattering	a)	Tilbakespredning fra bunnen
b)	Bottom reverberation	b)	Bunngjenklang
c)	Acoustic models	c)	Akustiske modeller
d)	Active sonars	d)	Aktiv sonar
e)	Measurements	e)	Målinger

THESAURUS REFERENCE:

8) ABSTRACT

Comparing the three bottom backscattering algorithms we observe variations in the resulting bottom reverberation levels from 0 to more than 20 dB in some cases. Concentrating on the variations at shorter to medium ranges where detection is limited by bottom reverberation we find that levels predicted by the McKinney & Anderson and del Balzo algorithms tend to produce equivalent results in many cases whereas the Lambert algorithm tend to produce higher levels at least for the harder bottoms. Turning to the cases where real sonar data are available, we observe that the McKinney & Anderson and del Balzo algorithms provide good agreement with the data in many cases whereas the Lambert algorithm generally predicts too high levels. It is observed that the agreement between model predictions and sonar data is clearly dependent on the correctness of the model assumptions, particularly the depth profile (flat bottom in our case) and the oceanographic conditions. Based on the simulations and the comparisons with real data it appears that for the cases studied the McKinney & Anderson algorithm is no less valid for the CAPTAS and Spherion frequencies than are the two other algorithms. We have seen that the McKinney & Anderson and del Balzo algorithms generate equivalent results in many cases, particularly when comparing with measured sonar data. As far as this study goes, we have found no reason to replace the McKinney & Anderson algorithm with neither the del Balzo algorithm nor the Lambert/TUS algorithm.

9) DATE	AUTHORIZED BY This page only	POSITION
12. September 2002	John-Mikal Størdal	Director of Research

ISBN 82-464-0683-3

UNCLASSIFIED

SECURITY CLASSIFICATION OF THIS PAGE
(when data entered)

CONTENTS

BOTTOM REVERBERATION PREDICTIONS WITH THE ACOUSTIC MODEL LYBIN:
A Comparison between three Bottom Backscattering Algorithms

1 INTRODUCTION

For a particular sonar and a set of environmental parameters the acoustic ray model LYBIN predicts transmission loss, reverberation and noise and probability of detection in a 2-D vertical section through the water volume. This vertical section is divided into 50x50 cells in range and depth, and the model contributions in each individual cell are integrated to produce average predictions for that cell. LYBIN predicts bottom reverberation from a bottom range cell by adding the contributions from all rays that hit the bottom within that bottom range cell.

The contributions to the resulting reverberation from each individual ray hitting the bottom are generated by an algorithm calculating what is termed the bottom backscattering coefficient. LYBIN is equipped with an empirical backscattering coefficient algorithm developed by McKinney and Anderson, see (1) and (2), which is based on measurement data from signals of frequencies higher than 12.5 kHz. This fact indicates that the algorithm should be valid for frequencies above 12.5 kHz only.

It is envisaged that LYBIN will be used to generate online predictions of sonar detection ranges onboard the Nansen class frigates. This function will be implemented by integrating LYBIN into the sonar tactical display. It is rather important that sub modules in a LYBIN model used for this purpose are valid for the Nansen class sonar frequency ranges. These frequency ranges are centred at 1.5 kHz and 6.5 kHz, considerably lower than 12.5 kHz. This is the reason for conducting this study where the McKinney and Anderson algorithm is compared at the lower frequency ranges mentioned above with two other algorithms, one due to del Balzo (1, 3) and the other a model used by THALES (1). Both algorithms are modifications of Lambert's rule, see section 2 below. The del Balzo algorithm is frequency independent, whereas the THALES algorithm is assumed to be valid over the frequency range 1-10 kHz.

In our simulations we have been using LYBIN version 3.3. This version does not accept different beam patterns in transmission and reception. Therefore a modified beam pattern had to be used in the simulations of the CAPTAS sonar.

2 THEORETICAL CONSIDERATIONS

2.1 General

Following active sonar transmissions in shallow water sound is reradiated from the surface and bottom interfaces and from inhomogeneities in the water volume. This reradiation of sound is called *scattering.* Scattering in direction of the (monostatic) receiver is termed backscattering. The sum of scattering contributions at the receiver is called *reverberation*. In this report we are concerned with *bottom backscattering* and *bottom reverberation*.

The fundamental ratio upon which reverberation depends is called *scattering strength.* It is the ratio, in decibel units, of the sound scattered by a unit area or volume, referred to a distance of 1 m, to the incident plane wave intensity. In our case we are concerned with bottom scattering from area elements.

The scattering strength is defined as:

$$SS = 10\log(I_{scat}/I_{inc})$$

$I_{scat} = I_s$ = scattered sound intensity
$I_{inc} = I_i$ = incident sound intensity

The function called Lambert's rule (or law) is a type of angular variation which many rough surfaces appear to satisfy for scattering of both sound and light. It is a simple algorithm governing the scattering from a surface element dA.
Lambert's rule predicts that the power of scattered sound in direction φ caused by a plane sound wave incident at an angle θ on an area element dA is given by the expression

$$P_s = I_s dA = \mu I_i (\sin\theta \sin\varphi) dA$$

I_s = intensity = P_s/dA (Watt/m^2)
μ = the Lambert constant
θ = angle with bottom of incident sound ray
φ = angle with bottom of scattered sound ray
dA = scattering area

When backscattering is considered, the angle φ equals angle θ, and the Bottom Backscattering Strength according to Lambert's rule is then

$$SS_B = 10\log\mu + 10\log\sin^2\theta$$

2.2 The Bottom Scattering Coefficient Algorithms

The initial source power associated with a ray is equal to the total transmitted power divided by the total number of rays. At a certain range from the source the ray power or intensity has been reduced by the beam pattern, reflection loss, attenuation, geometrical spreading etc. to the ray intensity which is incident on a bottom element.
The bottom scattering coefficient algorithm calculates the scattering contribution from each individual ray hitting the bottom. The power backscattered from the bottom area associated with a range cell is the sum of power contributions from all rays hitting the bottom inside that range cell. For a particular sonar and environmental situation the reverberation associated with a particular range cell is the power level at the receiver backscattered from that range cell. In the context of this report scattering is usually synonymous with backscattering.

The bottom scattering coefficient algorithms compared are

i) McKinney & Anderson
ii) del Balzo
iii) Lambert (TUS)

Detailed descriptions, formulas and plots of the functions can be found in reference 1.

i) The McKinney & Anderson (MKA) algorithm is an empirical function of bottom type, frequency and grazing angle, ie. the angle between the ray and the sloping bottom. (The function is described in more detail in reference 1). Basis for the model is the measurements reported in (2), measurements of backscattering strength as a function of grazing angle taken over the frequency range 12.5 – 290 kHz at 16 locations around the coast of the US. The model is obtained by fitting curves to the data and should therefore be assumed not to be valid outside the frequency range of the data.

ii) del Balzo's algorithm is a modified Lambert's rule which includes a correction term at low grazing angles (1). This correction term accounts for the effect that in some sediments there exists a scattering strength plateau caused by scattering inside the sediment. The model is a function of bottom type (grain size) and grazing angle and is frequency independent.

The rule is formulated as

$$\sigma_b(\theta) = \alpha(\varphi) + \mu(\varphi)*\sin^2\theta$$

$\alpha(\varphi)$ is the low gracing angle plateau, and both α and μ depend on the bottom type through the parameter φ. The parameter φ is related to mean sediment grain size δ in mm by $\delta = (1/2)^{\varphi}$.

iii) The Lambert/TUS algorithm (1) used by THALES is a function of gracing angle, bottom type (porosity) and frequency. This version of Lambert's rule is assumed to be valid for the frequency range 1 – 10 kHz. It is Lamberts'rule with the Lambert constant μ being a function of bottom type and frequency.

$$SS_B = 10\log\mu + 10\log(\sin^2\theta)$$

$$\mu = 0.84 f_{kHz} 10^{-\alpha}, \quad \alpha = 0.1(a+b*\text{porosity})$$

Values of α for some sediment types are

Sediment type	α
Mud	3.7
Sand	3.1
Rock	1.8

3 SIMULATIONS AND COMPARISONS

3.1 General

The various cases were simulated using LYBIN version 3.3. LYBIN 3.3 does not accept different beams in transmission and reception as does LYBIN 4.0. LYBIN 4.0 was not yet ready for use when the simulations reported here were conducted. To handle CAPTAS simulations we had to invent an intermediate beam pattern. Tests with LYBIN 4.0 after this version had become available showed changes in level but not much change in form of the simulated reverberation curves. The conclusions drawn in this report are not dependent on the approximations in beam pattern made.

The comparisons were conducted in the following way:
For each of the three Bottom Scattering Coefficient (BSC) algorithms all scenarios were simulated with all combinations of variables. Following each run the simulated probability of detection and transmission loss matrices and the reverberation arrays were recorded to file. Each case was then also recorded by copying the LYBIN screen to file and printer as a documentation of the visual POD differences (if any) between the three algorithms. Based

on given environmental and sonar input parameters, LYBIN calculates the three types of reverberation, surface- volume- and bottom-reverberation and noise. To compare the effects of the various BSC algorithms, the predicted bottom reverberation curves for the three algorithms are shown together in a plot, one plot for each scenario and parameter combination (see section 4 Results and Discussion, and Appendix B).

This comparison of curves will show whether or not there are significant differences between the algorithms, but will not give us any evidence as to the "correctness" of any of them. If we observe significant differences between the algorithms, this fact indicates that the algorithms are not equivalent. We will have to compare the LYBIN simulation results with measured sonar data to find out which algorithm is the best in terms of giving the best fit to real world data from a specific area. It is, however, not likely that one BSC algorithm will fit data from all areas.

For this report CAPTAS sonar measurement data are available from tests at Marstein 1998 (Mar98) and from Vestfjorden 2001 (the RUMBLE-test spring 2001), see section 4. Spherion data from Bjørnafjorden 1998 have been collected, but were not available for this report.

3.2 The variables

The variables in the simulations and comparisons have been

i) The three Bottom Scattering Coefficient algorithms

- McKinney and Anderson (abbreviated MKA or M)
- Del Balzo (abbreviated dBal or B)
- Lambert/TUS (abbreviated L)

ii) Three bottom types,

- hard bottom (LYBIN type 2, gravel/rock),
- medium hard bottom (LYBIN type 4, sand) and
- softer bottom (LYBIN type 8, silt/clay/mud)

iii) Two Nansen class sonars,

- the hull mounted Spherion, MRS2000 with one set of parameters for all cases, and
- the Combined activ/passive activated towed array system CAPTAS with two sets of parameters:
- CAPTAS_RUMBLE parameters as used in Vestfjorden in May 2001 have been used in all A-cases and B-cases,
- CAPTAS_MAR98 as used in the Marstein98 case for the Marstein location.

iv) Scenarios

Ten scenarios have been chosen, one idealised test-scenario with constant depth and sound velocity, and nine geographical locations with depth profiles and sound velocity profiles, measured or typical for the area and season. Locations with data available from previous sonar experiments were selected. These experiments have been conducted with sonars of the same make but older types compared with those to be installed on the Nansen class frigates. The CAPTAS sonar used had wider beams both in transmission and reception, and the SPHERION sonar had only half the bandwidth compared with the sonars to be installed on the new frigates.

A scenario depth profile can either be exact like the Bjørnafjorden example, or approximated to some ideal form like the A and B cases (see below) and the Lofoten and Marstein98 cases (flat bottom).

The areas A and B have been used by SACLANTCEN in their comparative study of transmission loss predictions produced by a number of underwater acoustic models, see (4) and (5). A is a deep location north-east of Madeira, and B is a more shallow area north-west of Iceland. Both areas are divided into three sub areas, one down-sloping, the other flat and the third up-sloping. All three bottom profile sub cases have been approximated to smooth profiles.

The scenarios have been:

Test case:	Depth 300 m, Range 10 km
Adown:	Depth (200 – 2200 m), range 22 km,
Aflat:	Depth 2200 m, range 22 km
Aup:	Depth (2200 – 200 m), range 22 km
Bdown:	Depth (160 – 500 m), range 22 km
Bflat:	Depth 500 m, range 22 km
Bup:	Depth (500 – 160 m), range 22 km
Vestfjorden01:	Depth 250 m flat, range 18 km
Marstein98:	Depth 272 m flat, range 30 km
Bjørnafjrd98:	Depth (0 – 500 m), range 5 km (MRS2000 only)

4 RESULTS AND DISCUSSION

4.1 General

The simulations and comparisons reported have been conducted to study the differences between the three bottom scattering coefficient algorithms in terms of the bottom reverberation predictions which they produce. It is of course also of interest to observe how well the bottom reverberation predictions correspond to real sonar signals recorded in areas of interest. Such measured signals have been available from Marstein98 and Vestfjorden01 for the CAPTAS sonar. In addition to the three types of reverberation predicted for the scenarios a constant (and low) background noise level has been introduced. Active sonar target detections are generally limited by the resulting reverberation at shorter and medium ranges, and by noise (ambient- and self noise) at longer ranges. The models have been compared at shorter to medium ranges where detection is limited by bottom reverberation and at somewhat longer ranges where detection is limited by volume reverberation. The choice of the scattering coefficient models becomes less important at longer ranges.

Results from the simulations selected for presentation are found as figures and line plots in Appendix B of this note. Three types of figures are presented:
Figures of type 1 are showing three line plots of bottom reverberation, one for each bottom type tested (a hard bottom (LYBIN bottom type 2) on top of the page, medium (type 4) in the middle and a softer bottom (type 8) below). Each line plot contains bottom

reverberation curves for the three BSC algorithms. Also shown is the (constant) background noise level (own ship- and ambient noise).
Figures of type 2 are showing
a) a copy of the LYBIN screen, each with the sound velocity profile used and three figures: Raytrace, Transmission Loss and Probability of Detection (POD) for the del Balzo BSC algorithm,
b) the POD plot for the Lambert BSC algorithms, and
c) the POD plot for the McKinney & Anderson BSC algorithm (always in this sequence).
The bottom type for all three cases is given in the Ocean parameter list found in the upper left part of the LYBIN screen (2, 4 or 8).
Figure type 3 is used to compare LYBIN predictions with real sonar data from the Vestfjorden01- and Marstein98 measurements. On each figure page are shown two different ping histories (Vestfjorden) or two different beam signals from the same ping (Marstein) for the actual bottom type (BT=2) found in the area. Also shown are estimates of volume reverberation, surface reverberation and background noise. Two plots per page as opposed to three have been used for the sake of clarity.

The simulation results are discussed in section 4.2 below. A limited number of scenarios have been shown. Intermediate cases have been excluded whereas cases showing least or most variability have been included. However, all cases studied have been included in two tables summing up the results of the simulations done for CAPTAS sonar frequencies (Table 4.1) and for SPHERION sonar frequencies (Table 4.2).

The results of comparisons with measured data are discussed in section 4.3.

4.2 The simulations

The purpose of the simulations conducted has been to compare the bottom reverberation simulations based on the three Bottom Scattering Coefficient algorithms to find out how different (or similar) these simulation curves are for the scenarios selected.
In the discussion of the results below we therefore concentrate on the observable differences or similarities. This is done in two ways, as a discussion of the example figures presented in Appendix B where some of the simulations (not all) are presented, and as a summing up of results from all the simulations (Table 4.1 and Table 4.2).

4.2.1 A test scenario

Figure 1 is different from the other simulation figures. It shows the three reverberation curves (level in dB as a function of range) over 10 km with constant sound velocity over depth and constant depth for one bottom type only, BT=4, for two wind speeds, 0 m/s and 7 m/s. The “test”sonar frequency was 3.5 kHz. The three algorithms produce very similar predictions of bottom reverberation at zero wind speed.
Also at 7 m/s wind speed are the predictions from the three BSC-algorithms quite similar.

4.2.2 CAPTAS activated towed array sonar simulations

(CAPTAS sonar parameters are not listed in this report).

The scenarios and corresponding simulation figures shown are:

Adown	Fig. 2 & 3
Aflat	Excluded
Aup	Fig. 4
Bdown	Fig. 5
Bflat	Excluded
Bup	Fig. 6 & 7
Vestfjorden01	Fig. 8 & 9
Marstein98	Fig. 10 & 11

As can be seen most of the simulation results at CAPTAS frequencies (1-2 kHz) are shown. Only the cases Aflat and Bflat have been excluded. These two scenarios have been omitted because the results for Aup and Bup turn out to be quite similar, but with some more variability. The difference in frequency between CAPTAS and the McKinney & Anderson frequency range is fairly large (1-2 kHz compared to above 12.5 kHz). The larger the difference in frequency the more likely it is to observe differences between the BCS algorithms.

The LYBIN-screen is shown for the A-cases in Fig. 3, the B-cases in Fig. 7, for Vestfjorden01 in Fig. 9 and for Marstein98 in Fig. 11.

<u>Adown:</u>
Figure 2 is a type 1 figure as described in section 4.1 above. It shows the bottom reverberation results for this scenario. For the softer bottoms and longer ranges where detection is limited by noise or volume reverberation and not bottom reverberation we observe large differences between the algorithms. At the shorter ranges where detection is bottom reverberation-limited and for a hard bottom (BT=2), Lambert (L) estimates up to 10 dB higher level than del Balzo (dBal) and McKinney & Anderson (MKA). For BT= 4 MKA & dBal are more than 10 dB above L around 9-10 km range.
For BT=8 MKA is more than 10 dB above L and dBal up to 10 km range. Figure 3 shows the LYBIN screen and POD figures for all three BSCs at BT=8 (soft bottom). In this case del Balzo and Lambert cover more or less the same POD area whereas MKA is obviously different. It is difficult to assess if detection performance is really affected.

<u>Aup:</u>
Figure 4 shows the resulting bottom reverberation curves for Aup. The biggest differences are seen at the longest ranges where noise tends to dominate. At shorter range the differences are seen to be above 12 dB at most with L dominating.

<u>Bdown:</u>
Figure 5 shows the bottom reverberation curves for Bdown. Again the biggest differences are for ranges where noise or volume reverberation will dominate. At shorter ranges the differences are generally small (but L is 5-10 dB above dBal and MKA at ranges R<5km for BT=2).

<u>Bup:</u>
Figure 6 shows bottom reverberation curves for Bup. At the reverberation limited ranges we observe differences up to 10 dB or more at the shortest ranges (BT = 2 & 4) , 5 dB at longer ranges. L produces the highest levels where bottom reverberation dominates.
Figure 7 is showing the Bup LYBIN screen and POD figures for all three BSCs algorithms for a medium hard bottom (BT = 4). The POD-figures are visibly different, but it is difficult to relate these differences to the differences in bottom reverberatioon.

Vesfjorden01:
Figure 8 shows bottom reverberation curves for the Vestfjorden01 scenario.
We observe high differences at levels below the noise, but also some differences at shorter ranges, particularly for BT=2 (hard bottom) where L exceeds the other 2 algorithms with up to 10 dB out to 10 km range. dBal and MKA are very similiar. Figure 9 is showing the LYBIN screen and POD figures for all three BSCs and a hard bottom BT=2. It is found in section 4.3 that a hard bottom gives the best fit to measured data.

Marstein98:
Figure 10 shows bottom reverberation curves for the Marstein98-simulations. At short ranges for BT=2 L is 10 dB above dBal and MKA decreasing towards zero at 18 km where the reverberation curves dive under the noise. For softer bottom conditions the differences are smaller except at the longer ranges below noise level.
Figure 11 is showing the LYBIN screen and POD figures for all three BSCs and a hard bottom BT=2. From section 4.3 is found that a hard bottom gives the best fit of simulated reverberation to the measured data.

Table 4.1 below summarizes the CAPTAS simulation results.

4.2.3 SPHERION MRS2000 hull mounted sonar simulations

(Spherion sonar parameters are not listed in this report).
Only some of the Spherion simulation results have been selected for presentation. This is because the frequency difference 6.5 kHz to 12.5 kHz is less pronounced than in the CAPTAS case.
We have chosen the results showing most variability. The chosen scenarios and corresponding figures are:

Adown	Fig. 12
Bup	Fig. 13
Vestfjorden01	Fig. 14
Bjørnafjorden1	Fig. 15 & 16

Adown:
Figure 12 shows bottom reverberation curves for Adown. The curves are quite similar to those presented for the CAPTAS case for a hard bottom, BT=2, except at ranges from 8 to 11 km where MKA is much higher than L and dBal. For softer bottom conditions (BT= 4 & 8) where MKA falls down below noise, L and dBal (and L only for BT=8) falls off 1 km further out. And near 12 km range for BT=4 L produces a peak 15 dB above noise, 500 m wide, whereas for BT=8 del Balzo (B) produces a peak of the same height and width.

Bup:
Figure 13 shows the bottom reverberation curves for Bup. For a hard bottom (BT=2) we observe some variation, 5-10 dB for the whole range 1 to 16 km. The softer bottom (BT=4) shows variations 5-10 dB in the range from 5 to 10 km and peaks above noise at longer ranges. The BT=8 curves are not much different for ranges below 4 km. Above 4 km where noise or volume reverberation dominate, the variability is great.

Vestfjorden01:
Figure 14 shows the bottom reverberation curves for the Vestfjorden01 scenario. We observe noticeable variations between the curves, particularly for BT=2 below 5 km and above 5 km for softer bottom conditions.

Bjørnafjorden1, 1998:
Figure 15 shows the bottom reverberation curves from Bjørnafjorden1. For the hard bottom (BT=2) and to some degree also for the softer bottom (4) we observe noticeable variability, up to 10 dB over the whole range (5km).
Figure 16 is showing the LYBIN screen and POD figures for the three BSC algorithms. We observe clear differences between the three POD plots. It seems that there could be some differences in detection performance between del Balzo and the other two algorithms since del Balzo is showing a higher POD in the mid part of the plot.

Table 4.2 summarizes the Spherion simulation results in the same way as described for Table 4.1

4.2.4 Summary of simulation comparisons

The comparisons tell us about the similarities or differences between the algorithms for the various cases simulated. Based on the fact that the three algorithms are valid at different ranges of frequency, the comparisons could give us some indications as to which BSC algorithms should be used or discarded for some of the cases simulated.

In Table 4.1 & Table 4.2 we have compared the reverberation levels from the three BSC algorithms for different sections of range. The ranges for which noise is greater than bottom reverberation, Noise > BotRev, are of little importance. The ranges where BotRev > Noise have been subdivided in three parts, Short, Medium and Long. The most important parts are now Short and Medium where detection is likely to be limited by bottom reverberation. Ranges Long are considered not so important since detection at these ranges most likely will be limited by volume reverberation or (variable) noise and not by bottom reverberation.

The three reverberation curves are then compared in pairs and classified in the following categories:

- almost Equal (Max dif<5 dB) (E = no or insignificant POD differences)
- Smaller differences (Max dif >= 5 & Av dif <= 10 dB) (S = some POD differences)
- Large differences (Av/max dif > 10/20 dB) (L = POD differences may be significant)

(Max dif = maximum difference within the sub range excluding single points and the shortest ranges where the reverberation level falls off with decreasing range.
Av dif = average difference within the sub range)
Av/max dif > 10/20 = Average difference > 10 dB or maximum difference > 20 dB)
(E means that the algorithms are equivalent, L that they are clearly different and S is intermediate)

Code: B = dBal=delBalzo, L = Lambert, M = MKA=McKinney & Anderson
BM = Comparison del Balzo – McKinney & Anderson
BL = Comparison del Balzo – Lambert
ML = Comparison McKinney & Anderson - Lambert

Table 4.1, CAPTAS frequencies:
B & M are Equal in more cases than B & L or M & L, and both Smaller and Large differences occur more often with B & L and M & L than with B & M. None of the three BSC algorithms appears to be clearly superior or inferior to the other algorithms.

Table 4.2, Spherion frequencies:
There seem to be no differences between B, L and M regarding occurrence of Equal and Smaller differences. When it comes to Large differences they occur more often with B & L and M & L than with B & M. None of the three BSC algorithms appear to be clearly superior or inferior to the other algorithms.

Run ID	Figures	Bottom Type	Short Range BM	BL	ML	Medium Range BM	BL	ML	Ranges in km Short Medium
AdownC50	2, 3	2	E	S	S	E	S	S	1 - 6, 6 - 10
		4	E	S	S	E	S	L	1 - 6, 6 - 10
		8	L	E	L	L	S	L	1 - 6, 6 – 10
AflatC50	-	2	E	L	S	E	L	L	4 -12, 12 - 20
		4	S	E	S	E	E	S	4 -12, 12 - 20
		8	S	S	E	S	S	S	4 – 12, 12 – 18
AupC50	4	2	E	L	S	S	S	E	4 – 14, 14 – 20
		4	S	E	S	-	-	-	4 – 14
		8	E	S	E	-	-	-	4 – 14
BdownC50	5	2	E	S	S	E	E	E	1 – 5, 5 – 8
		4	E	S	E	-	-	-	1 – 5
		8	S	S	E	-	-	-	1 – 2
BflatC50	-	2	E	L	L	E	S	S	1 – 6, 6 – 15
		4	S	E	S	-	-	-	1 – 5
		8	S	S	E	-	-	-	1 – 5
BupC50	6, 7	2	E	L	S	E	S	E	1 – 5, 5 – 12
		4	S	E	S	-	-	-	1 – 5
		8	S	S	E	-	-	-	1 – 5
Vestfj01C50	8, 9	2	E	S	S	E	S	S	1 –5, 5 – 11
		4	S	E	S	-	-	-	1 – 5
		8	S	S	S	-	-	-	1 – 5
Marstein98 C88	10, 11	2	E	S	S	E	S	S	1 – 6, 6 – 15
		4	E	E	E	-	-	-	1 – 6
		8	S	E	E	-	-	-	1 – 5

Table 4.1 Summary of all simulations at CAPTAS frequencies (f_c = 1.5 kHz)
The bottom reverberation prediction curves are compared in pairs to determine similarity or difference between:
BM = del Balzo/McKinney & Anderson
BL = del Balzo/Lambert
ML = McKinney & Anderson/Lambert
Similarity or differences are characterized in terms of
E = almost Equal (no or insignificant POD differences)
S = Some differences (smaller POD differences can be expected)
L = Large differences (POD differences can be significant)
(see section 4.2.2 for details)
C50 and C88: Depth of CAPTAS transducers in meters.

Run ID	Figures	Bottom Type	Short Range BM	BL	ML	Medium Range BM	BL	ML	Ranges in km Short	Medium
AdownS5	12	2	E	S	S	L	L	L	1 - 6,	6 - 11
		4	E	E	E	L	L	L	1 - 6,	6 - 9
		8	S	E	S	S	L	L	1 - 6,	6 – 8
AflatS5	-	2	S	S	L	S	L	S	3 - 6,	6 - 19
		4	S	L	S	E	E	E	3 - 6,	6 - 19
		8	E	L	S	S	E	S	3 – 6,	6 – 19
AupS5	-	2	S	S	L	S	S	S	3 – 6,	6 – 20
		4	S	L	E	S	E	S	3 – 6,	6 – 14
		8	E	L	S	E	E	E	3 – 6,	6 – 14
BdownS5	-	2	S	S	E	S	E	S	1 – 5,	5 – 10
		4	E	S	S	-	-	-	1 – 5	
		8	E	E	E	-	-	-	1 – 3	
BflatS5	-	2	S	S	E	S	S	S	1 – 5,	5 – 15
		4	E	E	E	S	S	S	1 – 5	
		8	E	E	E	-	-	-	1 – 4.5	
BupS5	13	2	S	S	E	S	S	S	1 – 4,	4 – 16
		4	E	E	E	S	S	S	1 – 4,	4 - 9
		8	E	E	E	-	-	-	1 – 4	
Vestfj01S5	14	2	S	L	S	S	S	S	1 –5,	5 – 15
		4	E	E	E	L	L	L	1 – 5,	5 - 12
		8	S	E	S	L	L	L	1 – 4,	4 - 6
Bjørnafj1_ 98S5	15, 16	2	S	S	S	-	-	-	1 – 5	
		4	S	S	S	-	-	-	1 – 5	
		8	S	S	S	-	-	-	1 – 5	
Bjørnafj2_ 98S5	-	2	S	S	E	-	-	-	1 – 5	
		4	S	S	S	-	-	-	1 – 5	
		8	E	E	E				1 – 5	

Table 4.2 Summary of all simulations at Spherion frequencies (f_c = 6.5 kHz).
The bottom reverberation prediction curves are compared in pairs to determine similarity or difference between:
BM = del Balzo/McKinney & Anderson
BL = del Balzo/Lambert
ML = McKinney & Anderson/Lambert
Similarity or differences are characterized in terms of
E = almost Equal (no or insignificant POD differences)
S = Some differences (smaller POD differences can be expected)
L = Large differences (POD differences can be significant)
(See sections 4.2.2 and 4.2.3 for details

4.3 **Comparison with measured data**

Measurement data are available from the Vestfjorden 2001 tests (figures 17 – 21) and the Marstein 1998 tests (figures 22-26).

4.3.1 Vestfjorden 2001

The RUMBLE Project Report from First Sea Trial from 28/05/2001 to 04/06/2001 (see reference 6) describes how the Vestfjorden 2001 tests were carried out. Two test areas were used, area A in the inner part of the fjord, and area B further out. The sonar look direction (broadside beam) was either across or along the fjord axis. In the simulations we have assumed a flat bottom which is believed to be a good approximation in the middle and along the fjord. The oceanographic conditions were fairly constant and stable. One sound speed profile for the whole area is expected to be a fairly good approximation.
We have chosen to present four sonar signal returns from area A and four from area B. Among the signals analysed we have picked signals with the best and worst agreement with the predictions. The agreement occurs at ranges 5 – 13 km. Outside these ranges detection is limited by volume reverberation and noise. At shorter range below 4-5 km the return signals are much lower than predicted. It looks as if the signals have been reduced in level or normalized at these shorter ranges. Data from Marstein 98 shows much higher signal levels at the shortest ranges.

Area A:
Figure 17 is a check on bottom type. Clearly bottom type 2 gives the best fit to the measured sonar data, and this applies not only to the ping shown, but to all pings analysed from both area A and B.
Figure 18 shows two signals from leg RSA01105, beam direction along the fjord. Ping 8 near the SE edge of area A does not fit the predictions too well. The signal fall-off with range is different from that of the predictions. Ping 25 is located closer to the middle of the fjord. The agreement with the predictions (delB & MKA) is seen to be better than for ping 8 from 5 to 13 km range. Lambert (L) has the same fall-off, but a higher (7-8 dB) level.
Figure 19 shows two signal returns from leg RSA01107, beam direction along the fjord. As with leg RSA01105 the signal near the middle of the fjord (ping 30) is more in line with the predictions (DelB & MKA) than ping 100 near the NW edge.

Area B:
Figure 20 shows 2 signal returns from area B. Ping 35 from leg RSB01106, beam direction along the fjord and located in the mid-section of the fjord, shows fairly good agreement with the predictions at ranges from 5 to 13 km (deB & MKA). Ping 100 from leg RSB01103, beam direction across the fjord and at the innermost edge of the area does not agree too well with the delB and MKA predictions whereas the L-predictions fit quite well in the range 7 –12 km. One might expect that the flat-bottom assumption is not justified for beam directions across the fjord, and this may be the reason for the disagreement with the delB & MKA predictions. What seems to make area B different from area A is the Lambert (L) predictions agreement with data. This is also found in the next figure 21.
Figure 21 shows two other signal returns from area B, both with beam direction along the fjord. Ping 80 of leg RSB01105, in the mid south-western part of the area, does not agree with delB & MKA predictions. Lambert on the other hand agrees quite well with the data in the range 7.5-12.5 km. We have no clear explanation for the observed differences between area A and area B.

Ping 50 from leg RSB01108, near mid fjord and along the fjord, shows good agreement with the predictions (5-13 km, delB & MKA) whereas L, 7 dB above at 6 km range, has a slightly steeper slope..

4.3.2 Marstein 1998

The Marstein 98 tests were conducted in open sea outside Marstein near Bergen in the fall of 1998. This is a fairly shallow coastal water area east of the Norwegian trench. The data presented comes from one run from North to South along the coast some 30 km from shore. Ship heading was 167º and ship speed 6 knots. For this analysis we have decided to present 8 beam signals from 4 ping transmissions, 4 signals from beams pointing towards land and 4 signals from beams pointing towards the open sea. We have decided to approximate the bottom conditions with a flat bottom of 272 m depth and bottom type 2 (hard bottom, gravel or rock). One sound speed profile only is available. The bottom type assumption is based on some bottom information. In the figures presented the predictions have been adjusted up or down to fit the open sea beam data. It has been considered that the important issue is to determine if the slopes match.
The best and worst cases are shown.

Figure 22 is a check on the bottom type assumption. As can be seen bottom type 2 is clearly the best guess. Figure 23 shows 2 beam signals from file B1_02_11, ping 1 from run DVB01, beam 144 pointing towards open sea and beam 48 pointing towards land. The bottom reverberation predictions coarsely fits the beam 144 signals from 3-4 to 15-16 km (delB & MKA). The Lambert (L) predictions lie considerably above at shorter ranges, and the gradient with range does not fit the data. At the longest ranges the predicted volume reverberation fits the data quite well. The disagreements observed may be due to Sound Velocity Profile (SVP) variations or the bottom not being flat. Looking at beam 48 (towards land) the disagreement is much clearer at ranges above 11-12 km, and this is most likely due to the fact that a flat bottom is not a good approximation towards land.
Figure 24 shows two beam signals from file B1_02_31, ping 27 after run start. Beam 120 points towards the sea and beam 48 towards the coast. For beam 120 the fit between predictions and sonar signal is excellent both at short, medium and long ranges (delB & MKA; not L). The bottom reverberation fits the data from 3-4 to 13 km and volume reverberation further up to 28 km. Beam 24 pointing in the opposite direction does not agree so well with the predictions at short and medium ranges.
Figure 25 shows two beam signals from file B1_04_21, ping 3 (about 13 km after start of run DVB01), beams 144 and 48. The fit is quite good for both beams (delB & MKA) except for a hump in the predicted bottom reverberation curve at 7 km which is not found in the data. (This hump was present in the data shown in figure 24, beam 120.)
Figure 26 shows two beam signals from file B1_05_11, ping 1, (ping no.23 after the ping shown in figure 25).
Both beam signals match quite well with the bottom reverberation predictions out to 13 km range (delB & MKA). At longer ranges where volume reverberation limits detection, the data show more than 10 dB higher levels than predicted. This could be caused by biological matter (fish) that may upset the assumptions governing the volume reverberation predictions.

5 CONCLUSION

Comparisons between the three bottom backscattering algorithms are showing variations in the resulting bottom reverberation levels from 0 to more than 20 dB in cases at shorter ranges. Even more variability is found at longer ranges where detection is limited by noise rather than by reverberation. This variability is of little importance since it does not influence detection.

Concentrating on the variations at shorter to medium ranges where detection will be limited by bottom reverberation we observe that the levels predicted by the McKinney & Anderson and del Balzo algorithms tend to produce equivalent results in many cases, whereas the Lambert algorithm tend to produce higher levels at least for the harder bottoms. When observing the probability of detection predictions corresponding to the bottom reverberation simulations we find differences also here, but they are not so pronounced. The hardest bottom generally shows more POD variability between the BSC algorithms than do the softer bottoms. This applies to both sonar types and all scenarios.
Turning now to the cases where real sonar data are available, we observe that the McKinney & Anderson and del Balzo algorithms provide good agreement with the data in many cases whereas the Lambert algorithm generally predicts too high levels. It is observed that the agreement between model predictions and sonar data is clearly dependent on the correctness of the model assumptions, particularly the depth profile (flat bottom in our cases) and the oceanographic conditions.

Based on the simulations and comparisons with real data, it appears that for the cases studied the McKinney & Anderson algorithm is no less valid for the CAPTAS and Spherion frequencies than are the two other algorithms. We have seen that the McKinney & Anderson and del Balzo algorithms generate equivalent results in many cases, particularly when comparing with measured sonar data. As far as this study goes, we have found no reason to replace the McKinney & Anderson algorithm with any of the two other algorithms tested.

Acknowledgements

Many thanks go to Elin M. Dombestein for contributing the programs needed to extract and present the measurement data from the Marstein 98 tests.

References

(1) T.Jenserud, "RUMBLE Project. Scattering Index Models," FFI/Rapport–2001/03685

(2) C.M.McKinney and C.D.Anderson, "Measurements of Backscattering of Sound from the Ocean Bottom, " J.Acoust.Soc.Am. 36(1): 158-163, January 1964.

(3) D.R.Del Balzo, J.H.Leclerce and M.J.Collins, "Critical Angle and Seabed Scattering Issues for Active-Sonar Performance Predictions in Shallow Water," In *High Frequency Acoustics in Shallow Water*, SACLANTCEN Conference Proceedings Series CP- 45, 1997.

(4) C.M. Ferla and F.B. Jensen, "Performance Assessment of Propagation Models in AESS-6.0" SR-309, Saclant Undersea Research Centre, La Spezia, Italy, August 1999.

(5) C.M. Ferla, C. Isoppo, G. Martinelli and F.B. Jensen, "Performance Assessment of the LYBIN-2.0 Propagation-loss Model", SM-384, Saclant Undersea Research Centre, La Spezia, Italy, May 2001.

(6) Alain Plaisant, TMS, FR & Johnny Dybedal, KDA, NO, "RUMBLE Project Report from First Sea Trial from 28/05/2001 to 04/06/2001", Stjørdal, Norway 07/06/2001

APPENDIX

A FIGURES

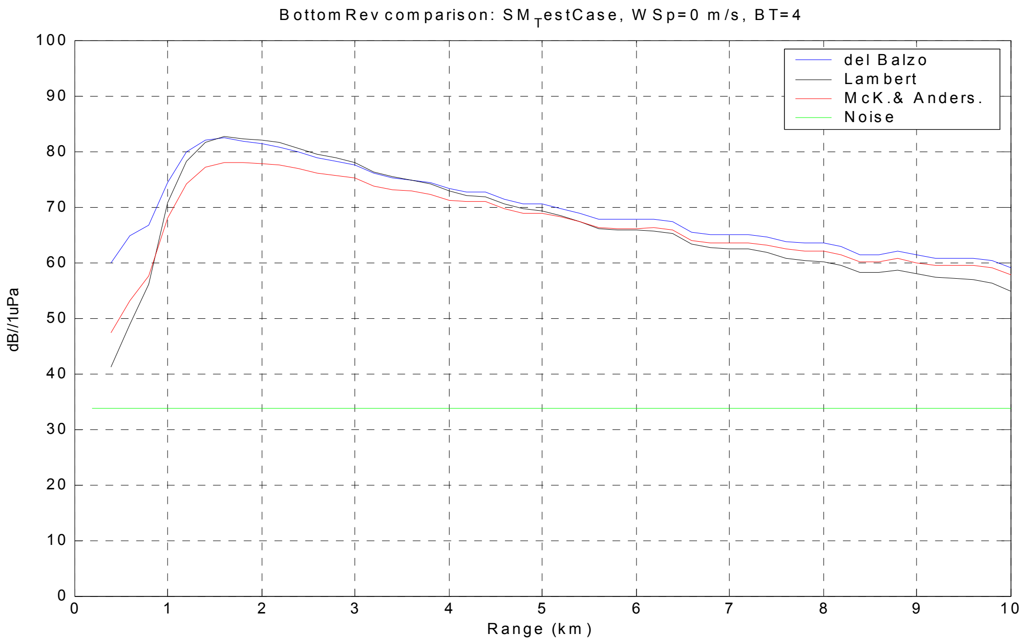

a) Wind speed 0 m/s

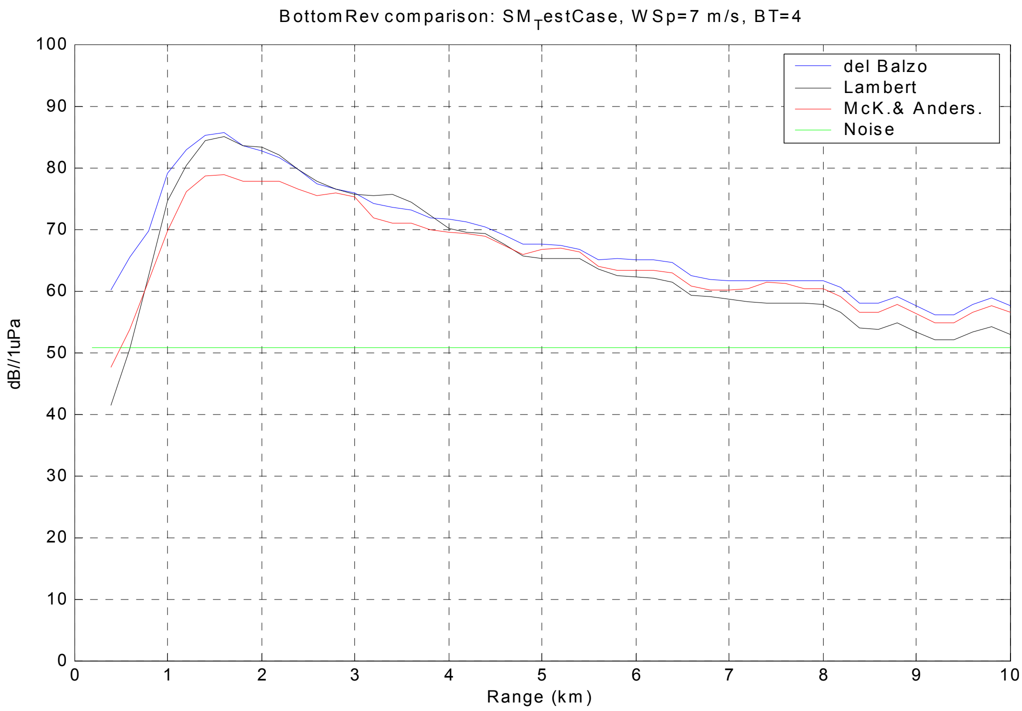

b) Wind speed 7 m/s

Figure A.1 Comparison between BSC algorithms for a test case with constant sound speed over depth and constant water depth with range

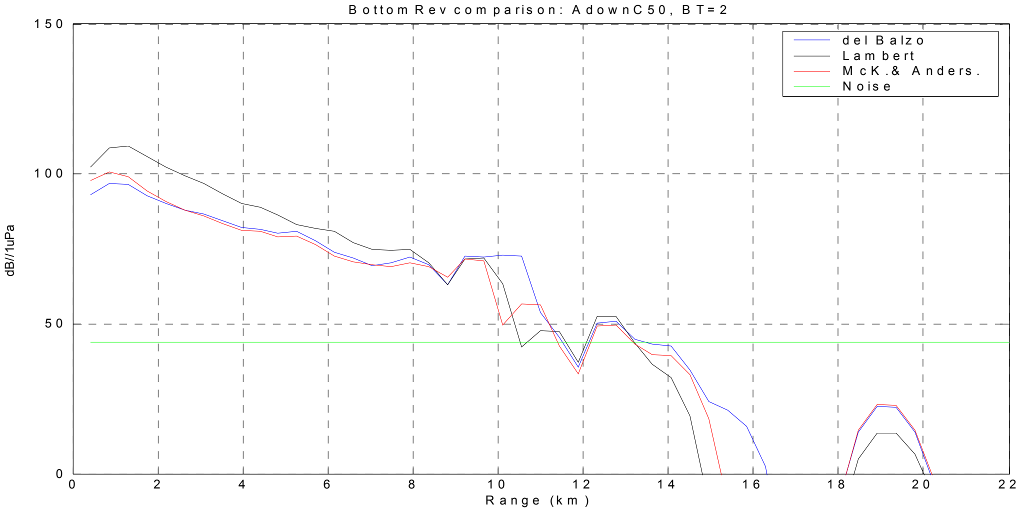

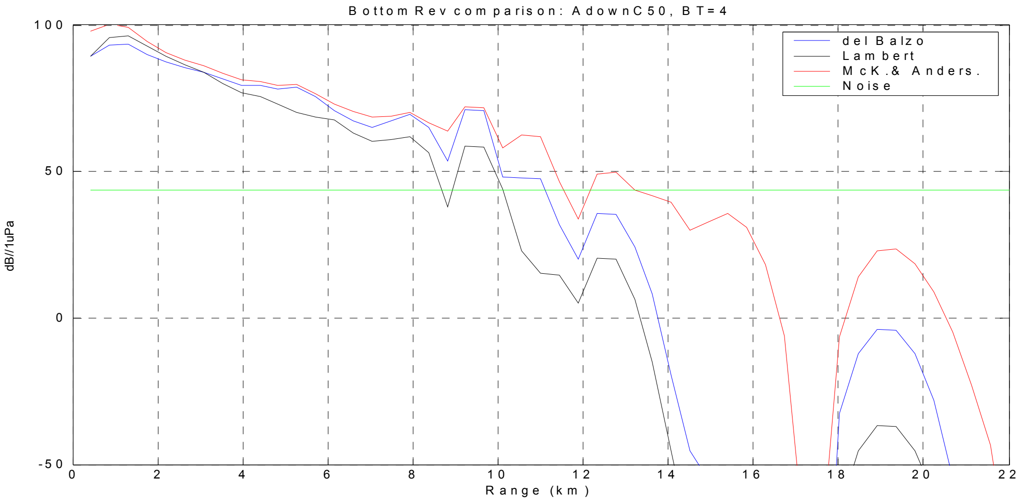

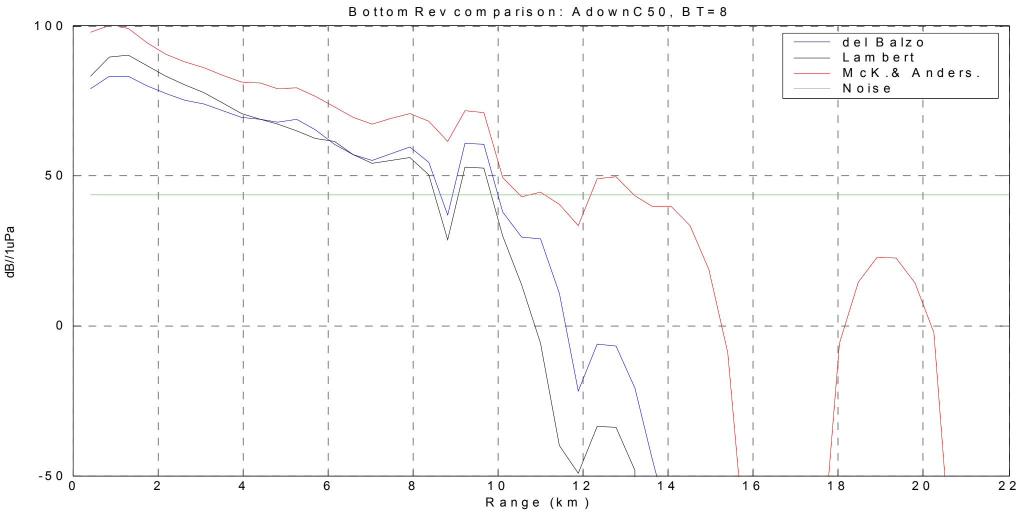

Figure A.2, Bottom Reverberation, Bottom Type 2 (hard), 4 (medium), 8 (soft)
AdownC50, CAPTAS sonar at 1.5 kHz, all Bot.Scat.Coef.models

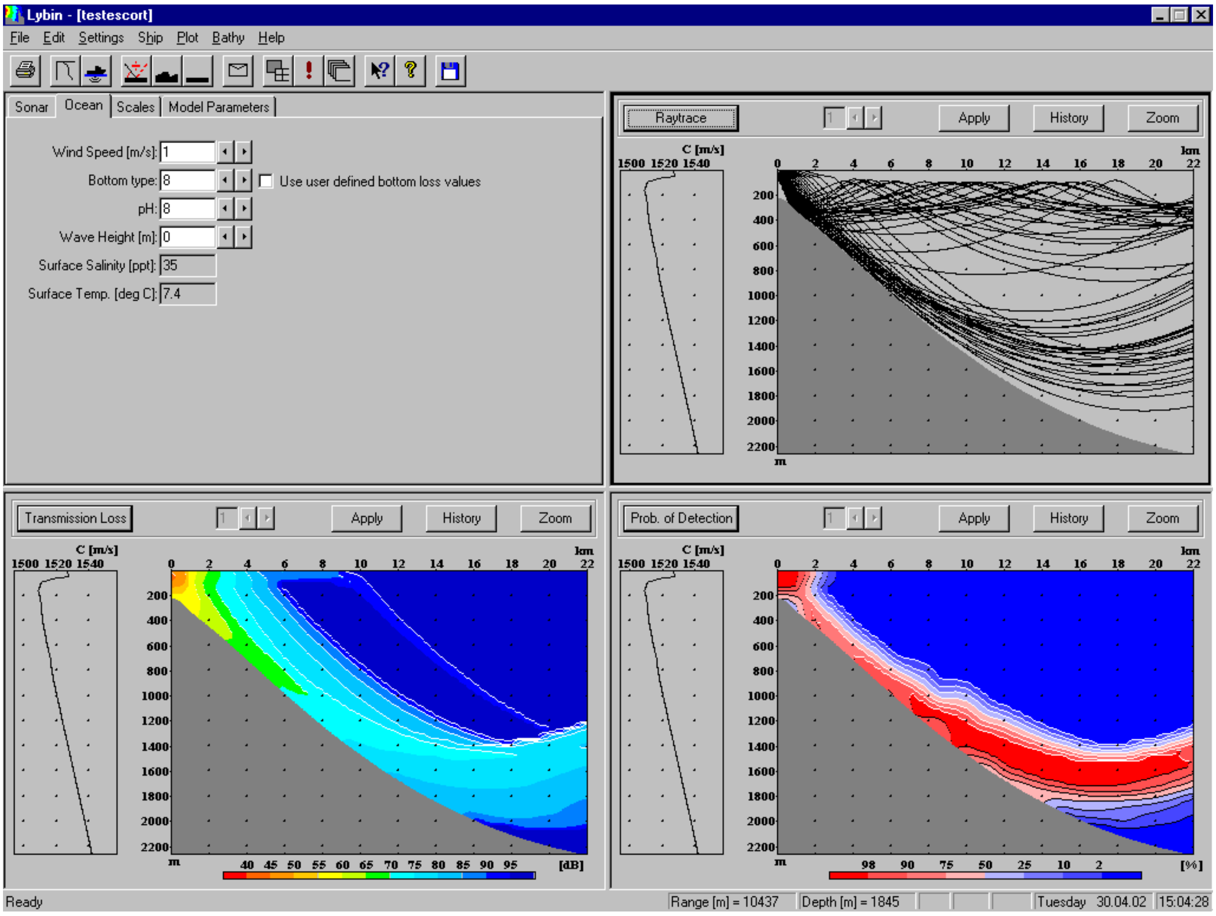

a) The LYBIN screen showing sound speed profile, Raytrace, Transmission Loss and Probability of Detection (POD) with del Balzo Bottom Scattering Coefficient algorithm.

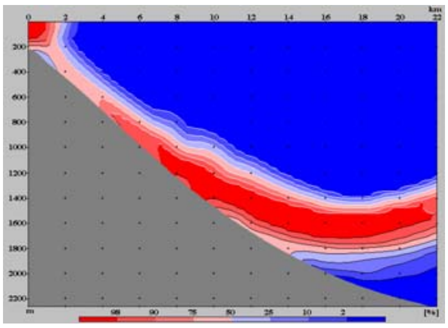

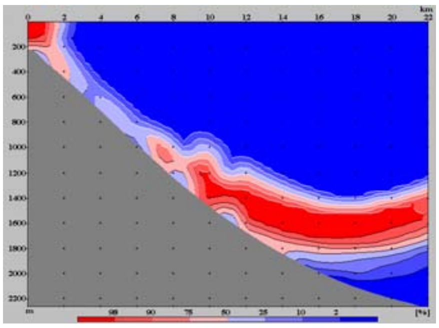

b) POD with Lambert/TUS BSC algorithm

c) McKinney and Anderson BSC algorithm BSC

Figure A.3 LYBIN simulations for scenario Adown: A comparison between all three BSC algorithms for CAPTAS frequencies (1.5 kHz) and bottom type 2 (hard, sand/rock)

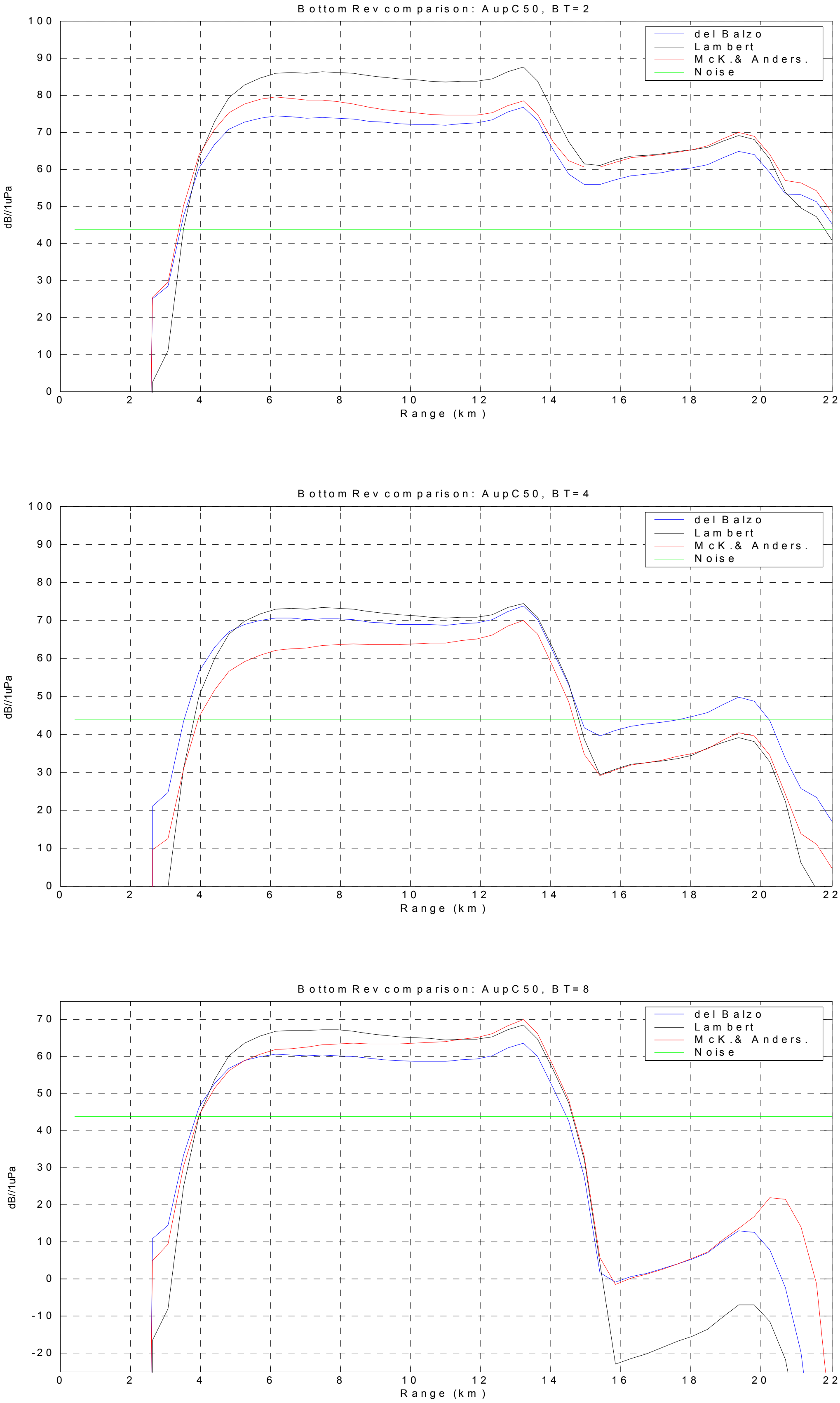

Figure A.4 Bottom Reverberation, Bottom Type 2 (hard), 4 (medium), 8 (soft)
AupC50, CAPTAS sonar, 1.5 kHz, all Bot.Scat.Coef.models

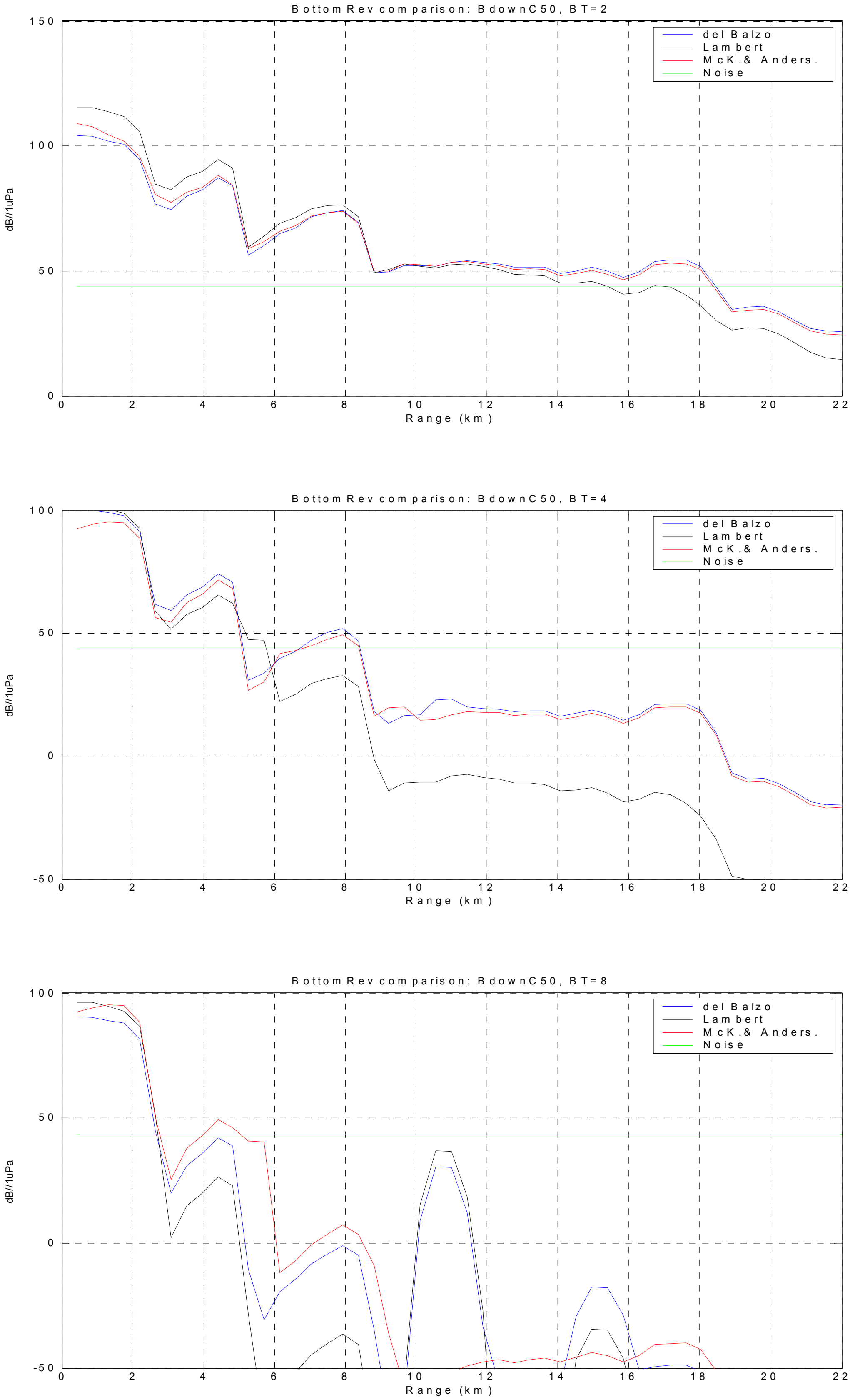

Figure A5 Bottom Reverberation, Bottom Type 2 (hard), 4 (medium), 8 (soft)
BdownC50, CAPTAS sonar, 1.5 kHz, all Bot.Scat.Coef.models

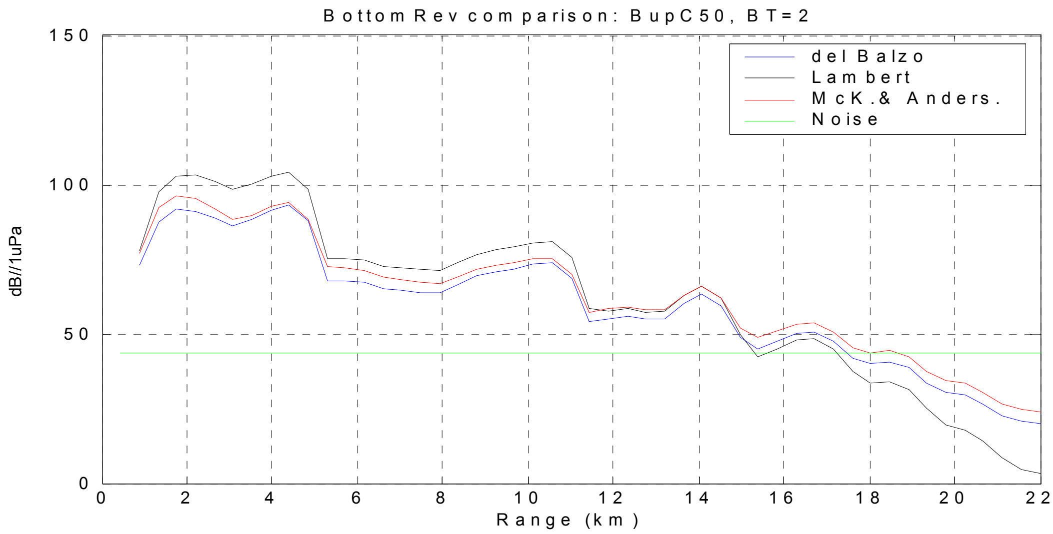

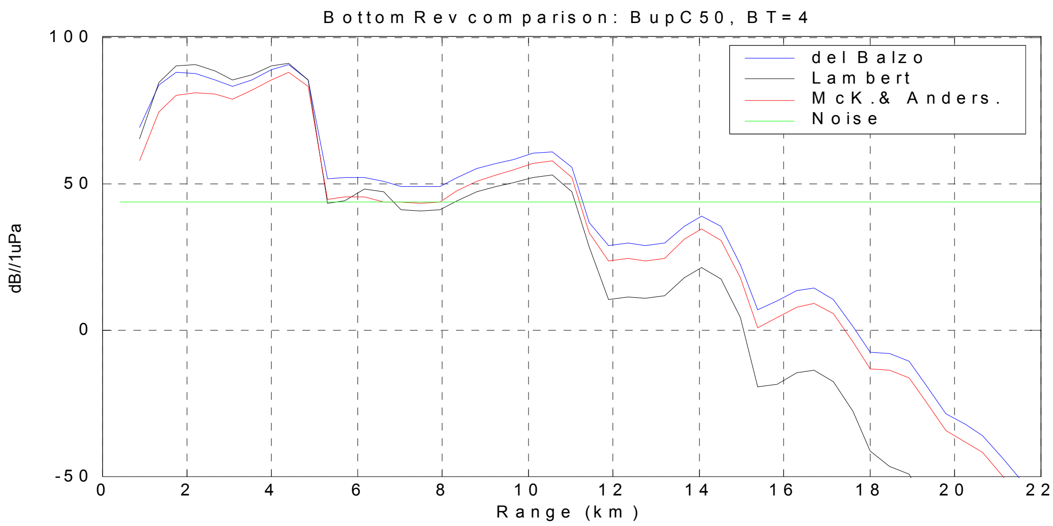

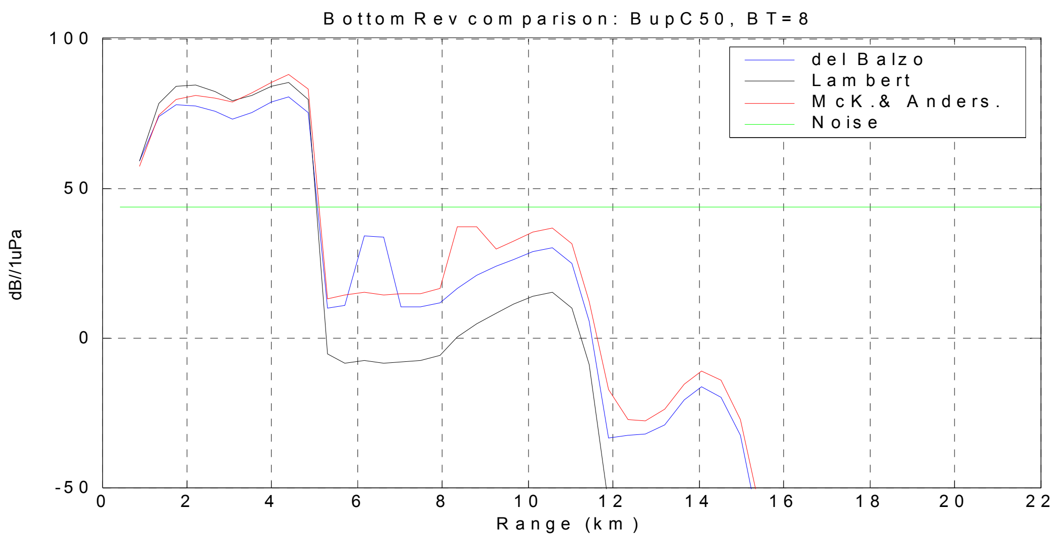

Figure A.6 Bottom Reverberation, Bottom Type 2 (hard), 4 (medium), 8 (soft)
BupC50, CAPTAS sonar, 1.5 kHz, all Bot.Scat.Coef.mpdels

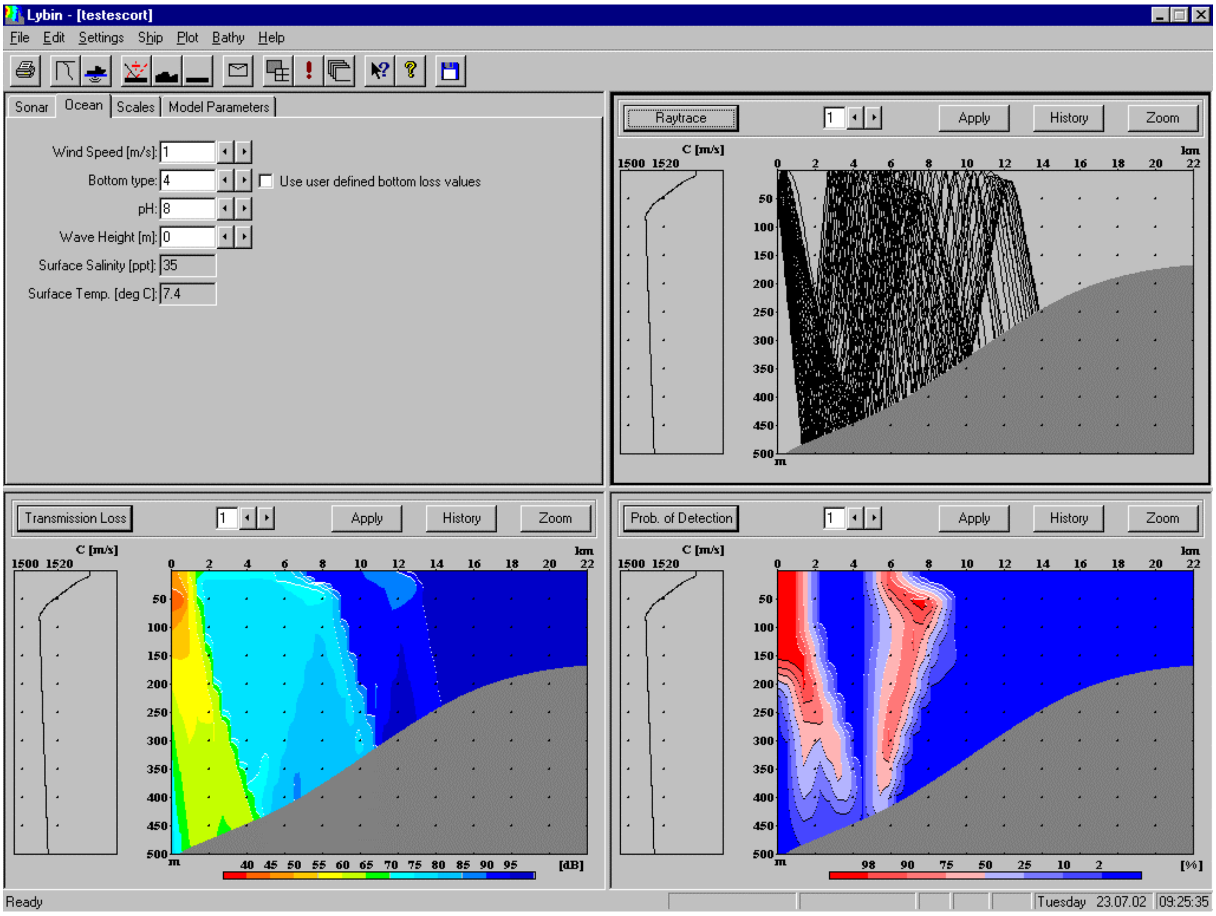

a) The LYBIN screen showing sound speed profile, Raytrace, Transmission Loss and Probability of Detection (POD) with the del Balzo Bottom Scattering Coefficient algorithm.

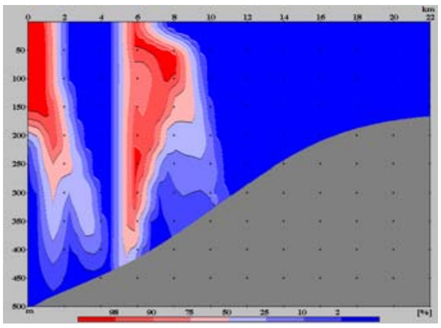

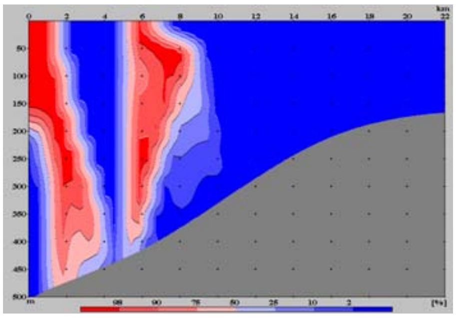

b) POD with the Lambert/TUS BSC algorthm

c) POD with the McKinney & Anderson BSC algorithm

Figure A.7 LYBIN simulations for scenario Bup: A comparison between all three BSC algorithms for CAPTAS frequencies (1.5 kHz) and bottom type 2 (hard, sand/rock).

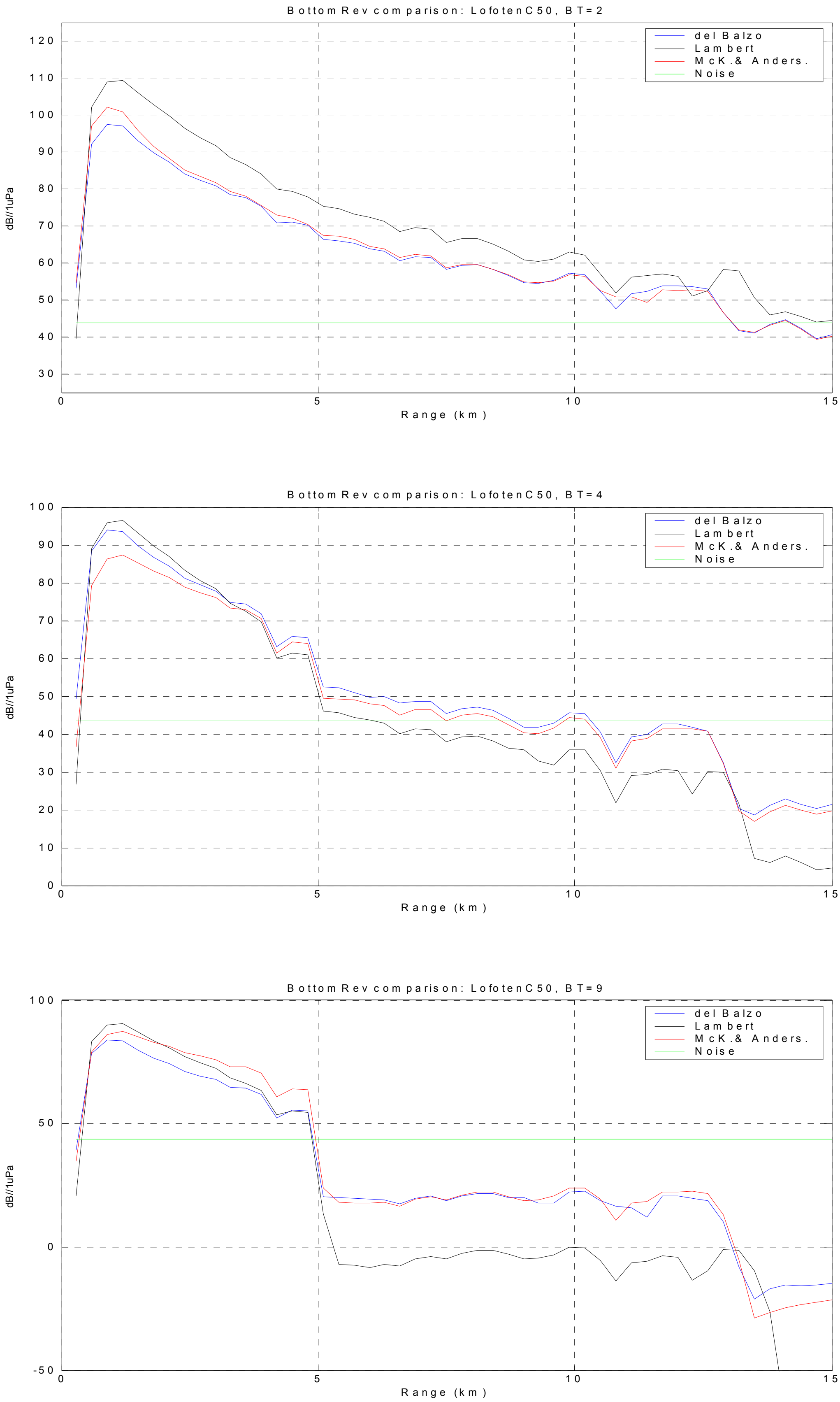

Figure A,8 Bottom Reverberation, Bottom Type 2 /hard), 4 (medium), 9 (soft)
Vestfjorden01C50, CAPTAS sonar, 1.5 kHz, all Bot.Scat.Coef.models

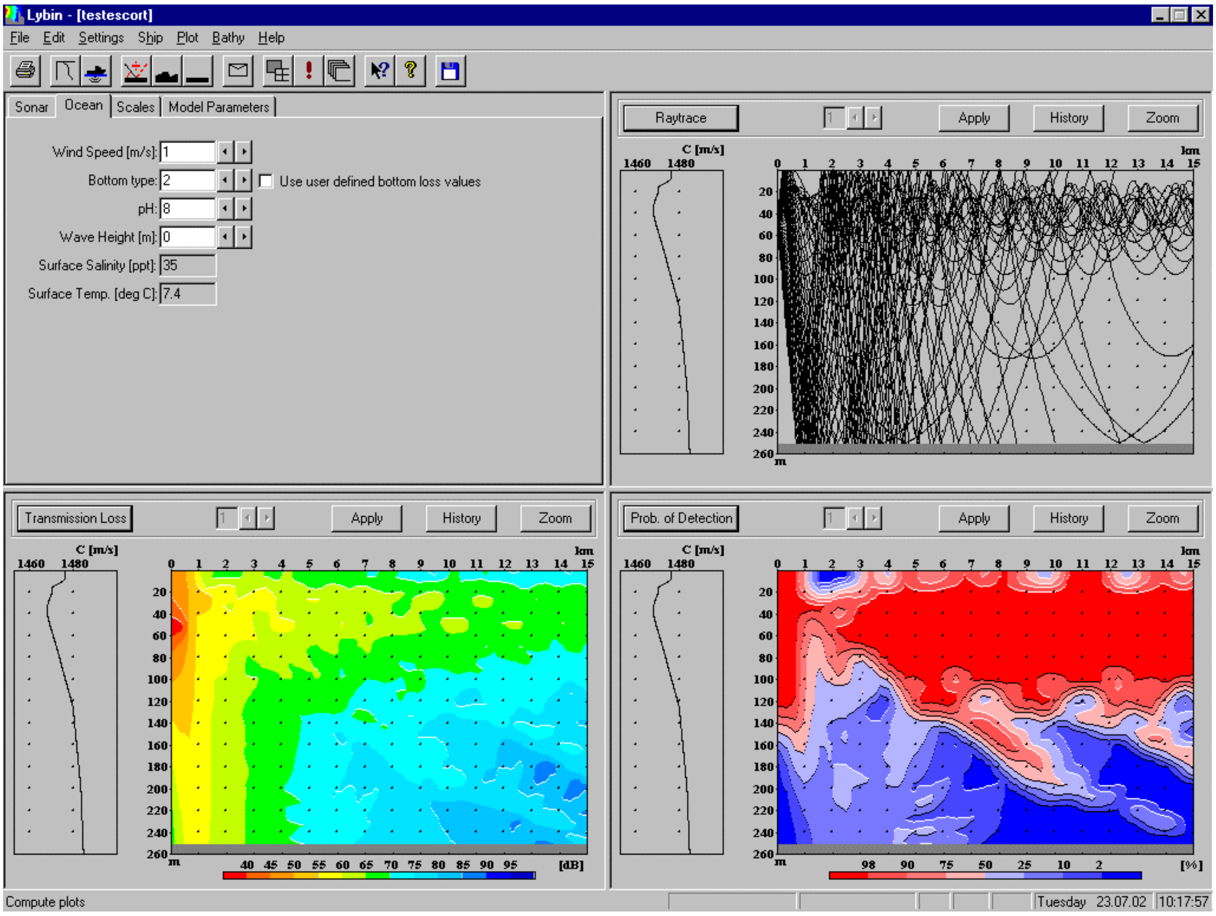

a) The LYBIN screen showing sound speed profile, Raytrace, Transmission Loss and Probability of Detection (POD) with the del Balzo Bottom Scattering Coefficient algorithm.

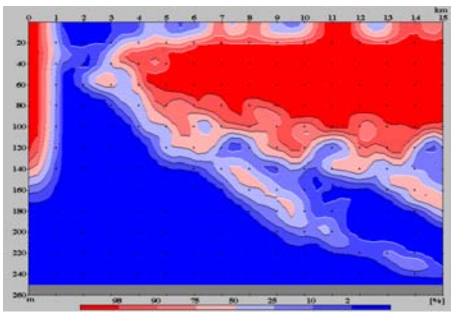

b) POD with the Lambert/TUS BSC algorithm

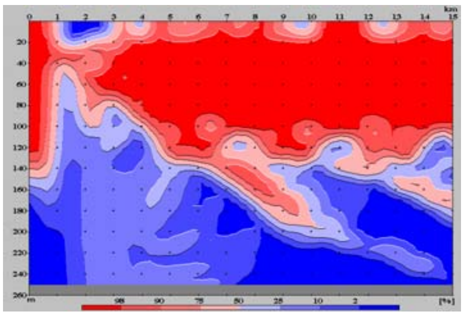

c) POD with the McKinney & Anderson BSC algorithm

FigureA. 9 LYBIN simulations for scenario Vestfjorden01: A comparison between all three BSC algorithms for CAPTAS frequencies (1.5 kHz) and bottom type 2 (hard, sand/rock)

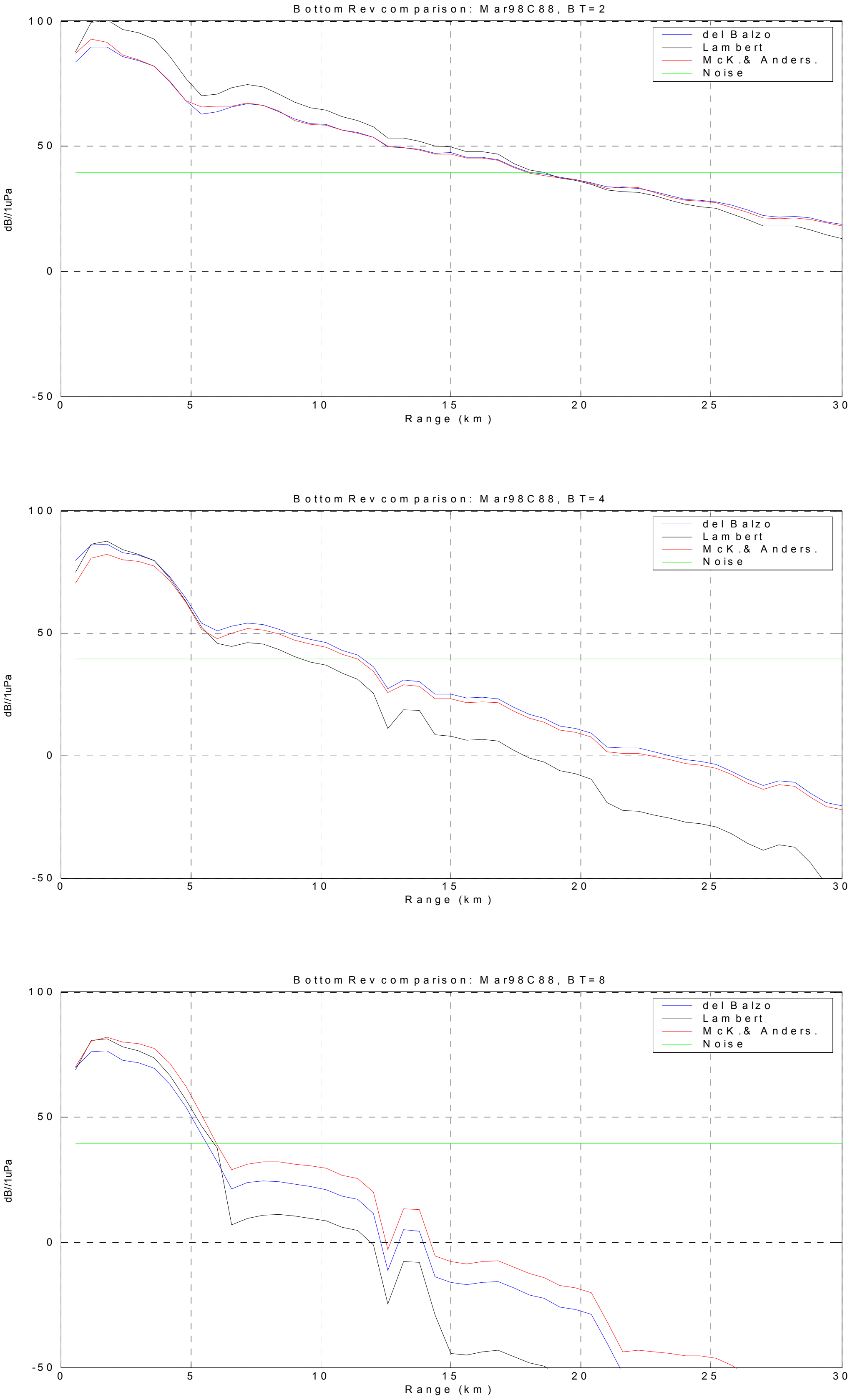

Figure A.10 Bottom Reverberation, Bottom Type 2 (hard), 4 (medium), 8 (soft)
Mar98C88, CAPTAS sonar, 1.5 kHz, all Bt.Scat.Coef.models

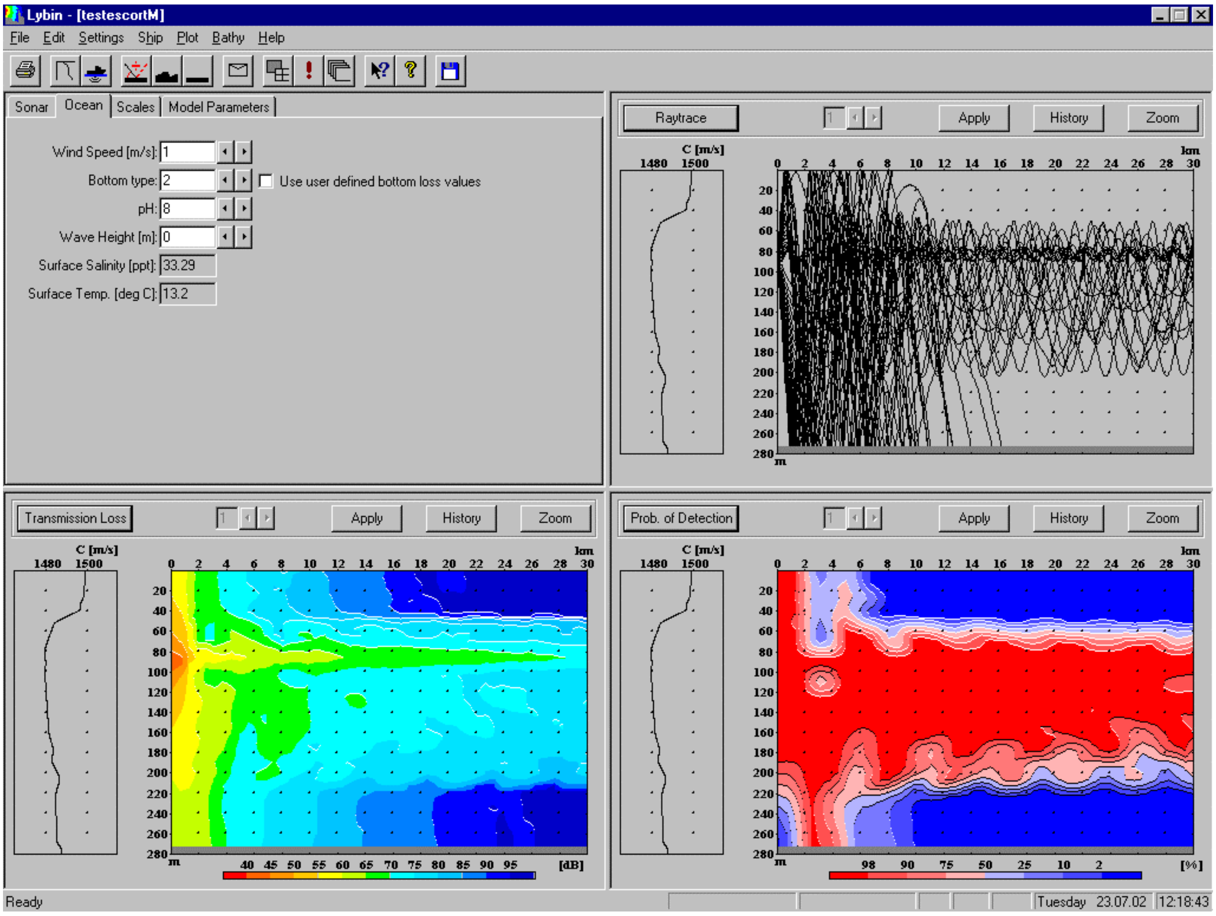

a) The LYBIN screen showing sound speed profile, Raytrace, Transmission Loss and Probability of Detection (POD) with the del Balzo Bottom Scattering Coefficient algorithm

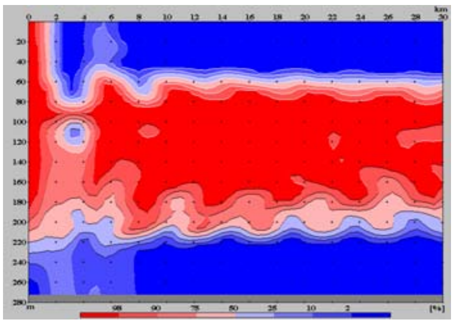

b) POD with the Lambert/TUS BSC algorithm

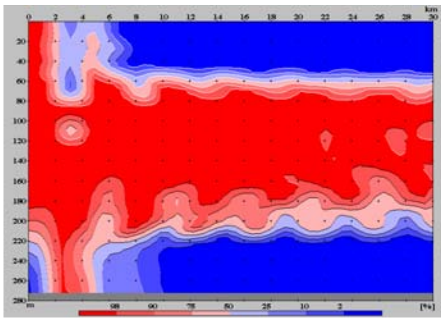

c) POD with the McKinney & Anderson BSC algorithm

Figure A.11 LYBIN simulations for scenario Marstein98: A comparison between all three BSC algorithms for CAPTAS frequencies (1.5 kHz) and bottom type 2 (hard, sand/rock

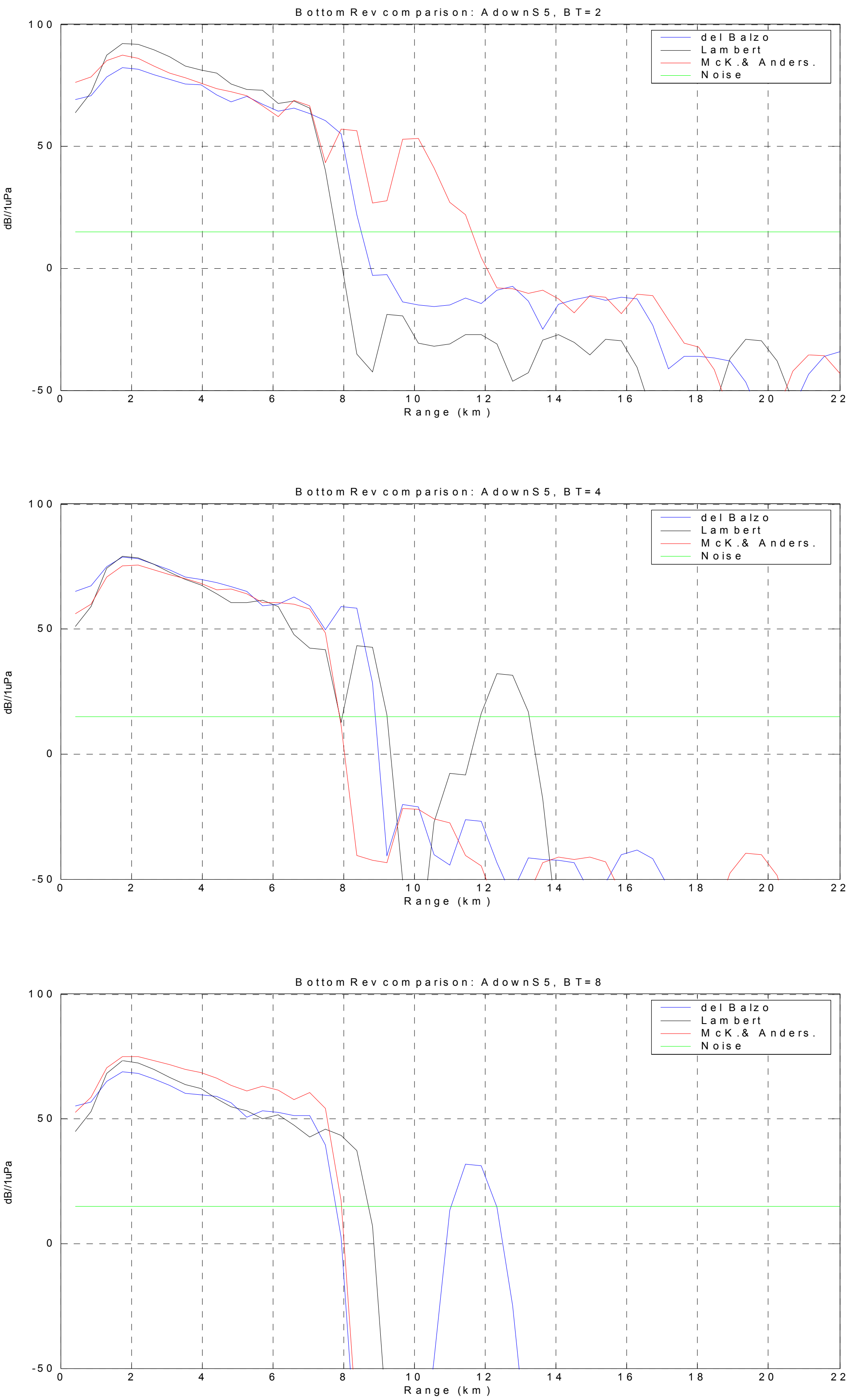

Figure A.12 Bottom Reverberation, Bottom Type 2 (hard), 4 (medium), 8 (soft)
AdownS5, MRS2000 sonar at 6.5 kHz, all Bot.Scat.Coef.models

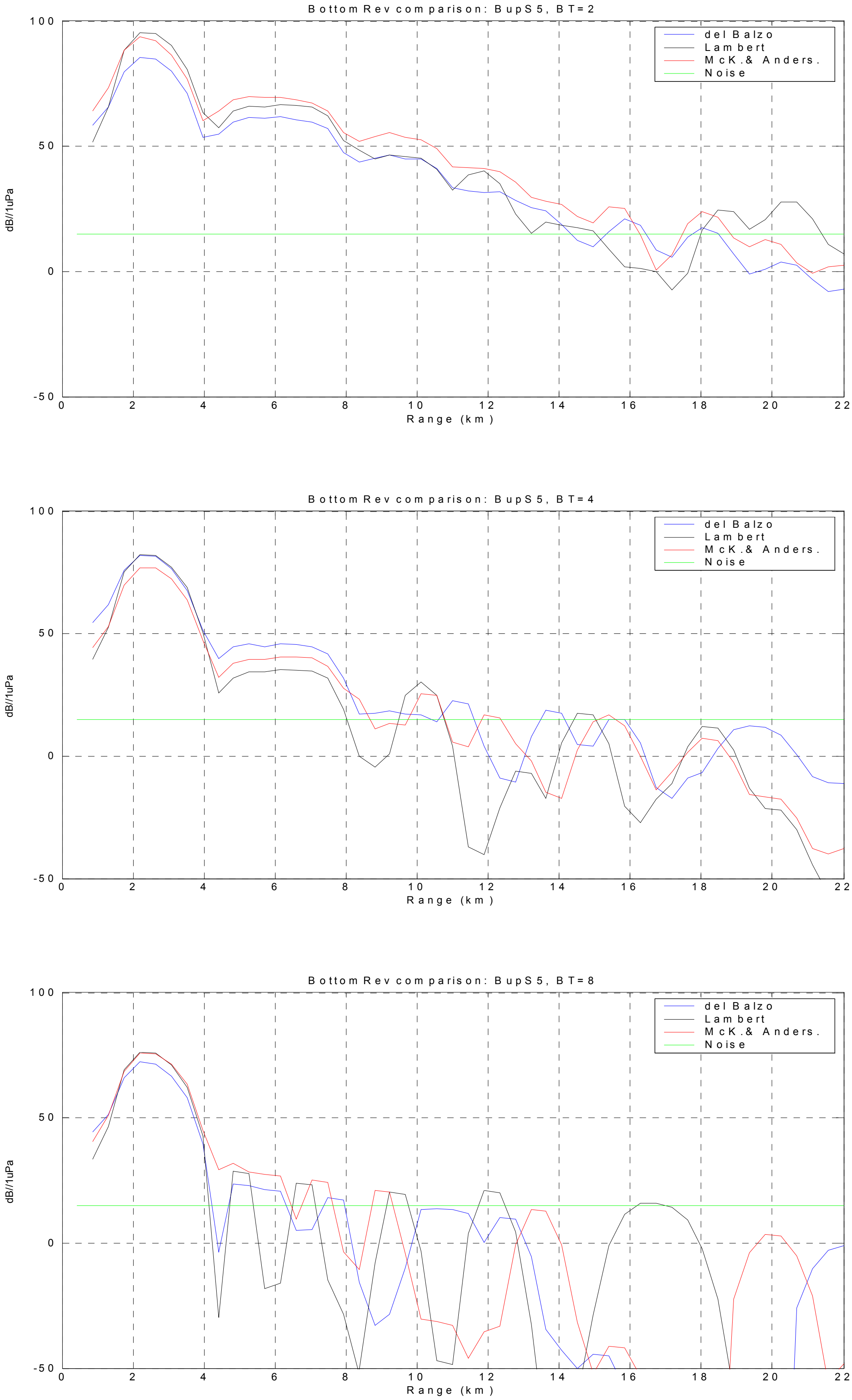

Figure A.13 Bottom Reverberation, Bottom Type 2 (hard), 4 (medium), 8 (soft)
BupS5, MRS2000 sonar, 6.5 kHz, all Bot.Scat.Coef.models

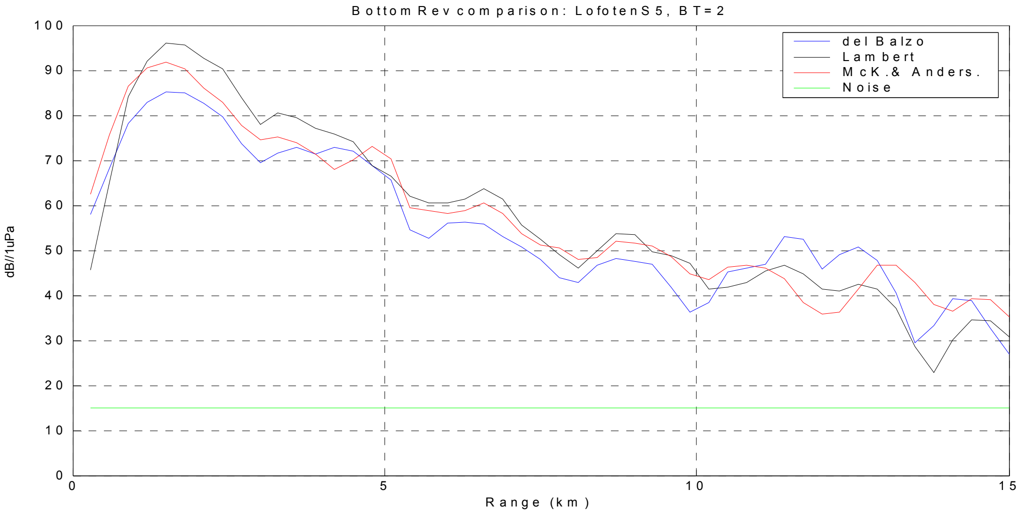

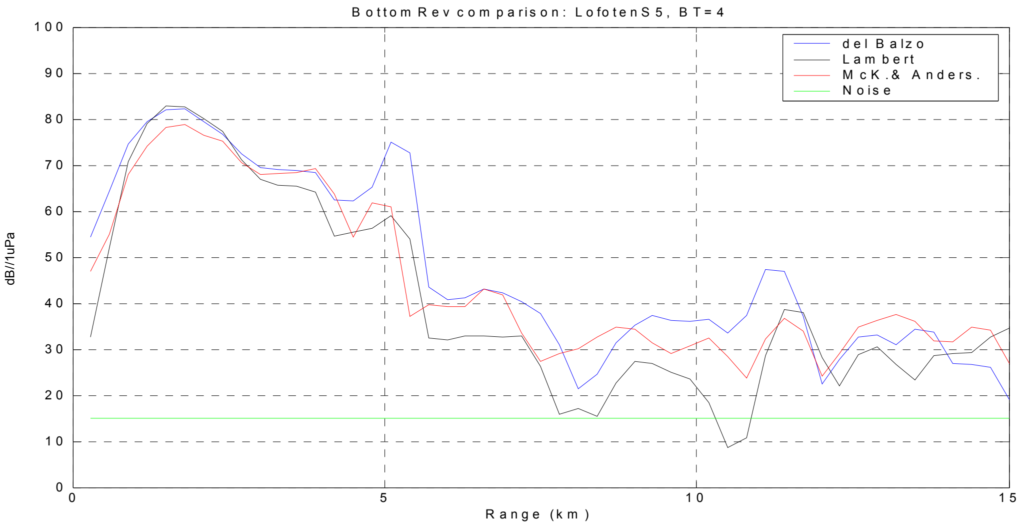

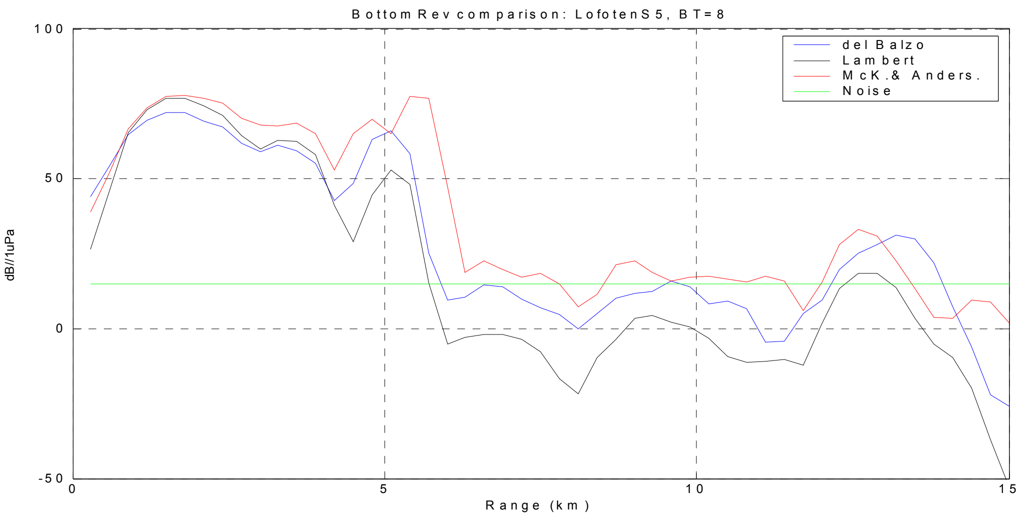

Figure A.14 Bottom Reverberation, Bottom Type 2 (hard), 4 (medium), 8 (soft).
Vestfjorden01S5, MRS2000 sonar, 6.5 kHz, all Bot.Scat.Coef.models

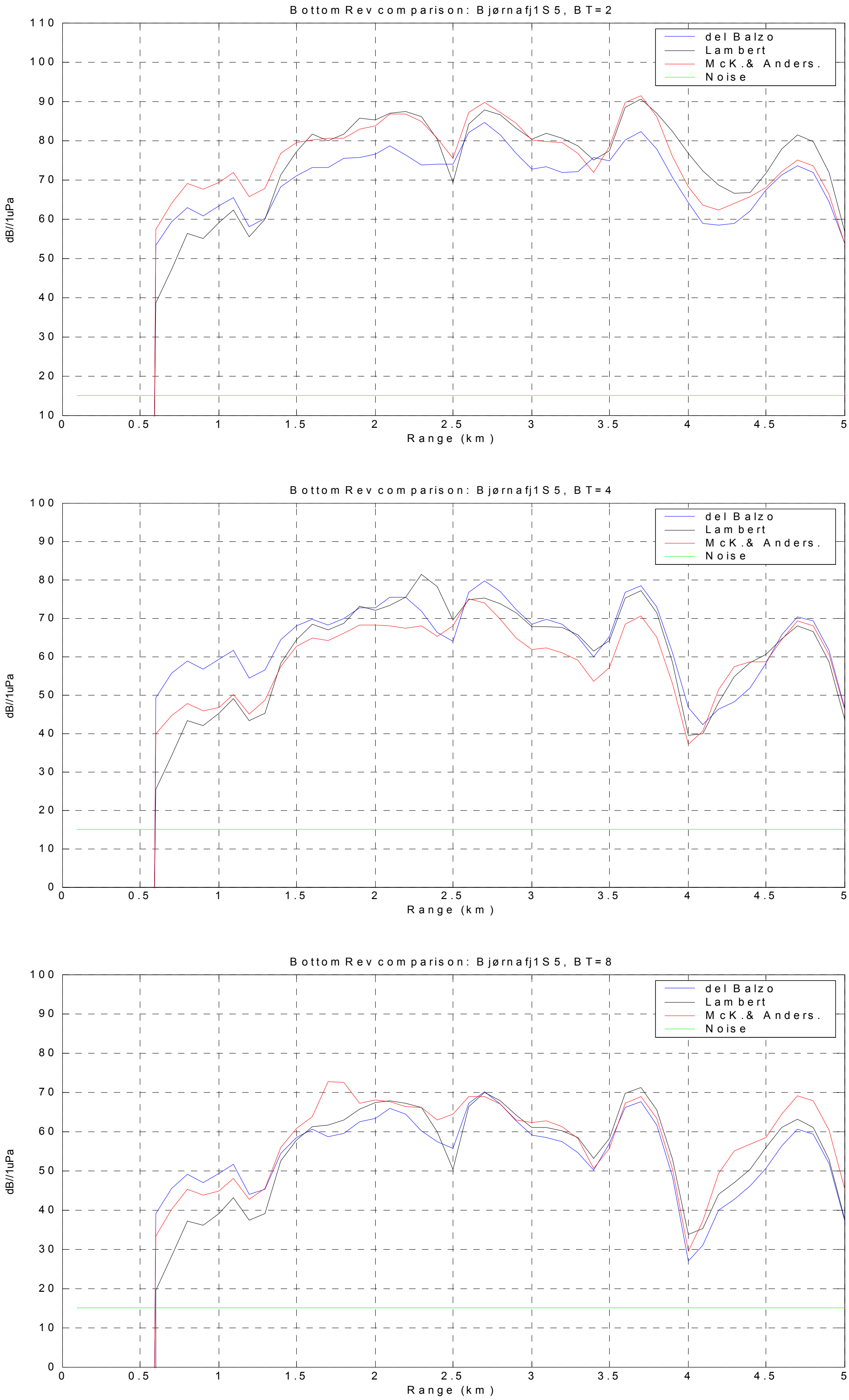

Figure A.15 Bottom Reverberation,Bottom Type 2 (hard), 4 (medium), 8 (soft)
Bjørnafj.1S5, MRS2000 sonar, 6.5 kHz, all Bot.Scat.Coef.models

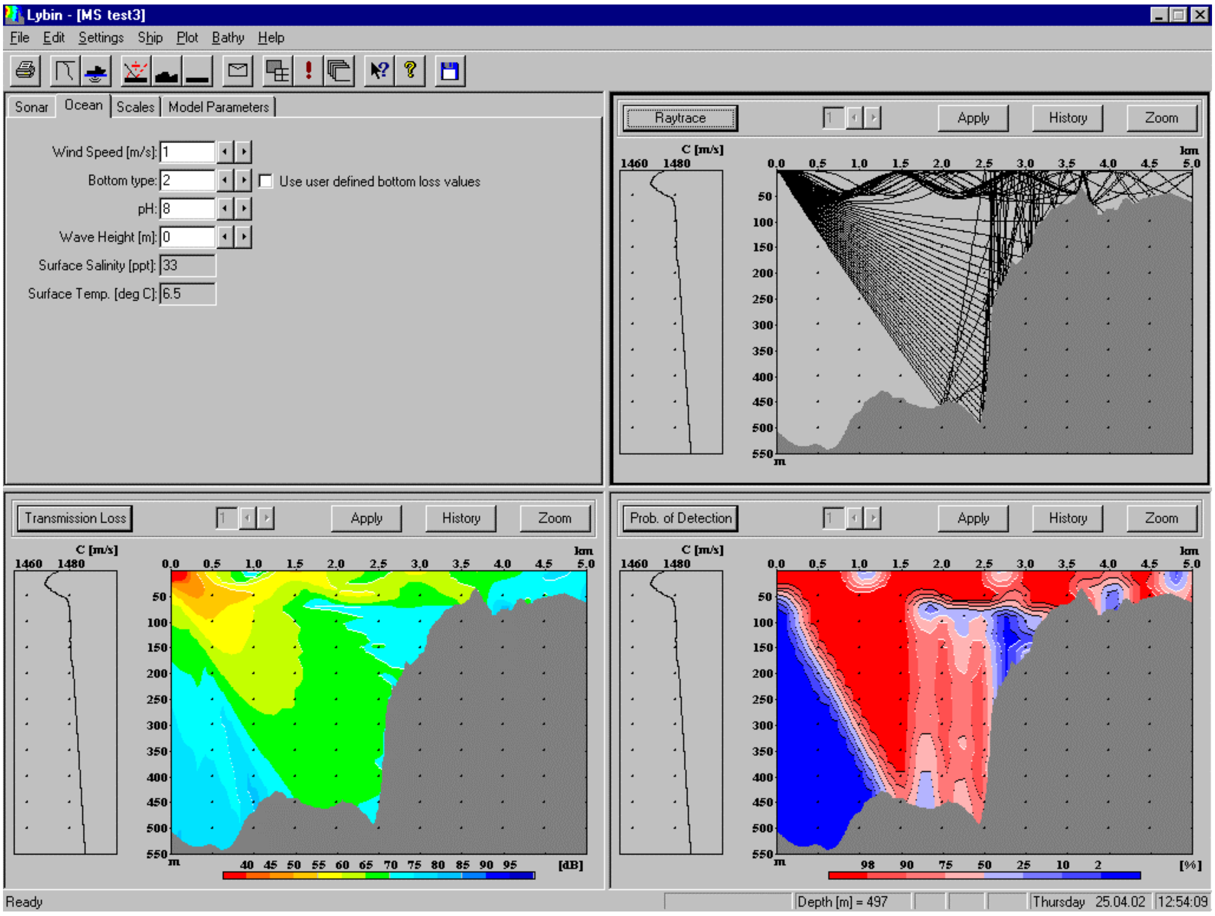

a) The LYBIN screen showing sound speed profile, Raytrace, Transmission Loss and Probability of Detection (POD) with the del Balzo Bottom Scattering Coefficient algorithm

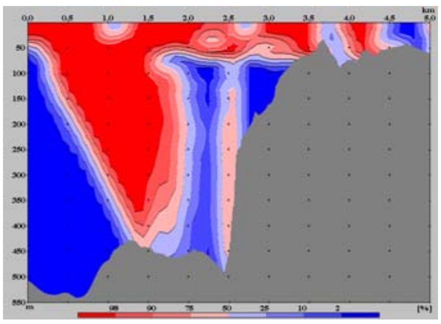

b) POD with the Lambert/TUS BSC algorithm

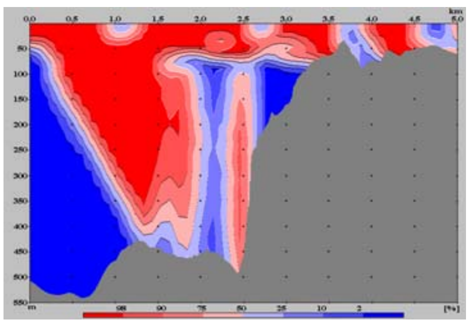

c) POD with the McKinney & Anderson BSC algorithm

Figure A.16 LYBIN simulations for scenario Bjørnafjorden1 1998: A comparison between all three BSC algorithms for Spherion frequencies (6.5 kHz) and bottom type 2 (hard, sand/rock)

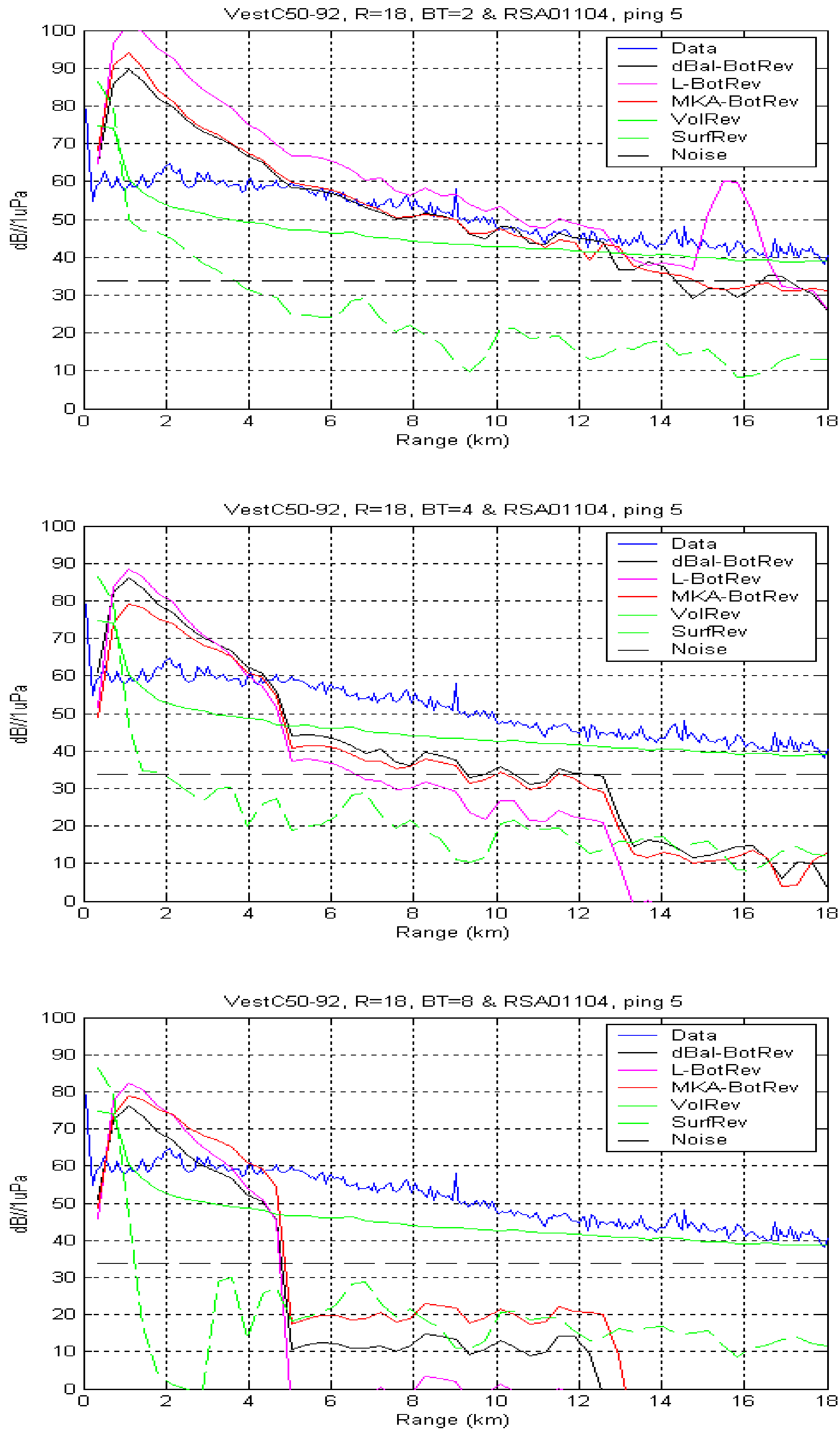

Figure A.17 Ping no. 5 from run no. RSA01104 compared with simulated background for bottom types BT = 2, 4 & 8. The best fit is clearly for BT=2

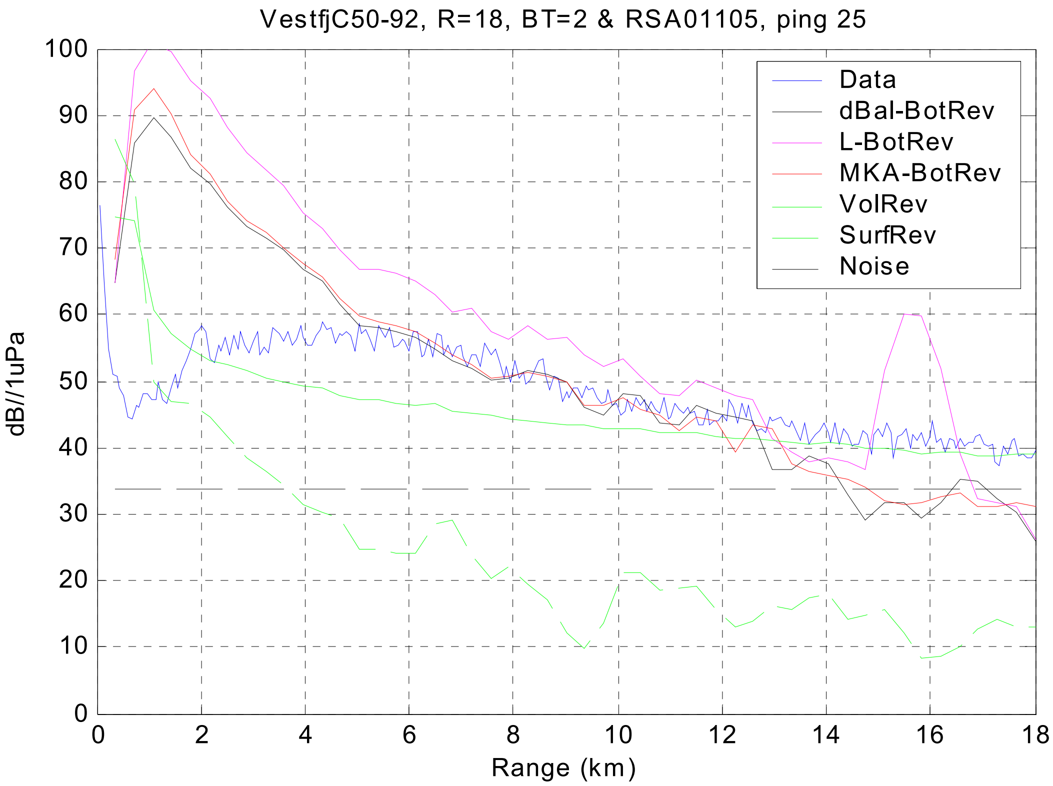

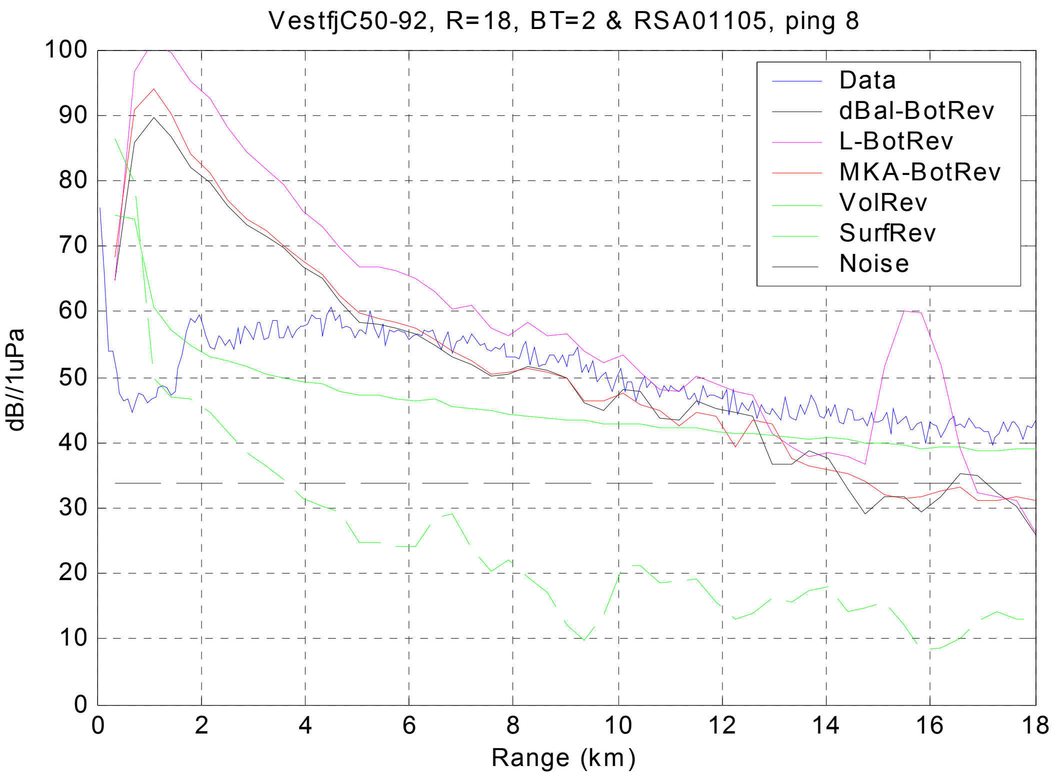

Figure A.18 Bottom reverberation variability is shown in sonar returns from 2 different pings from run 1, area A in Vestfjorden.

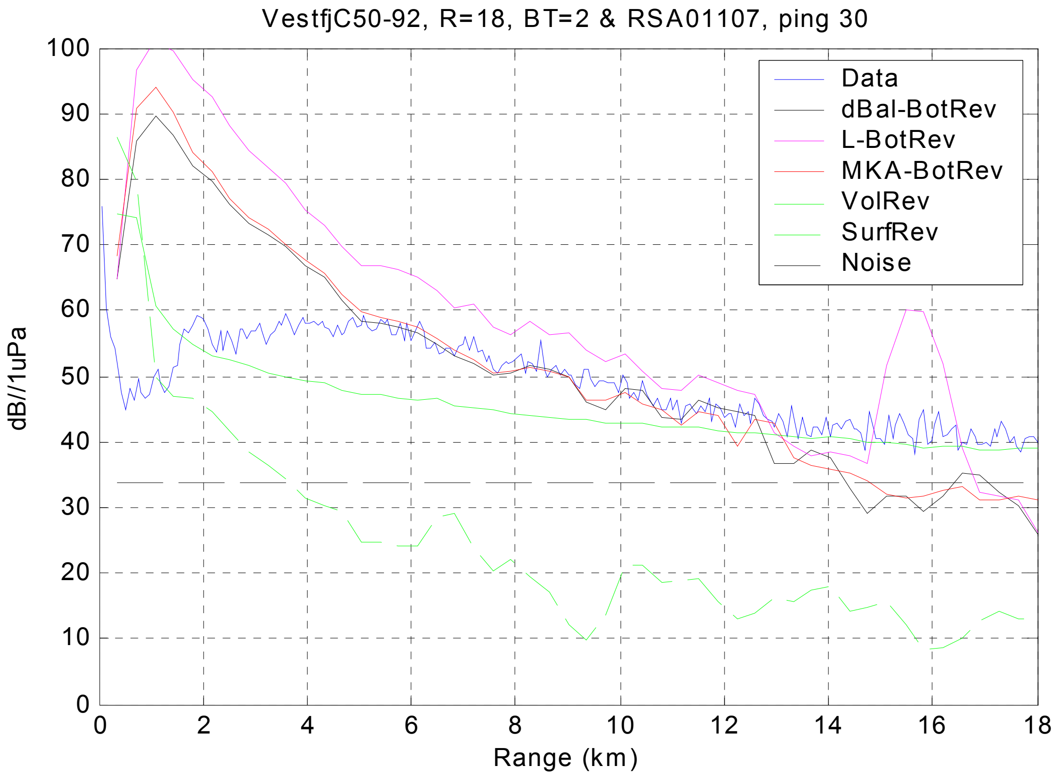

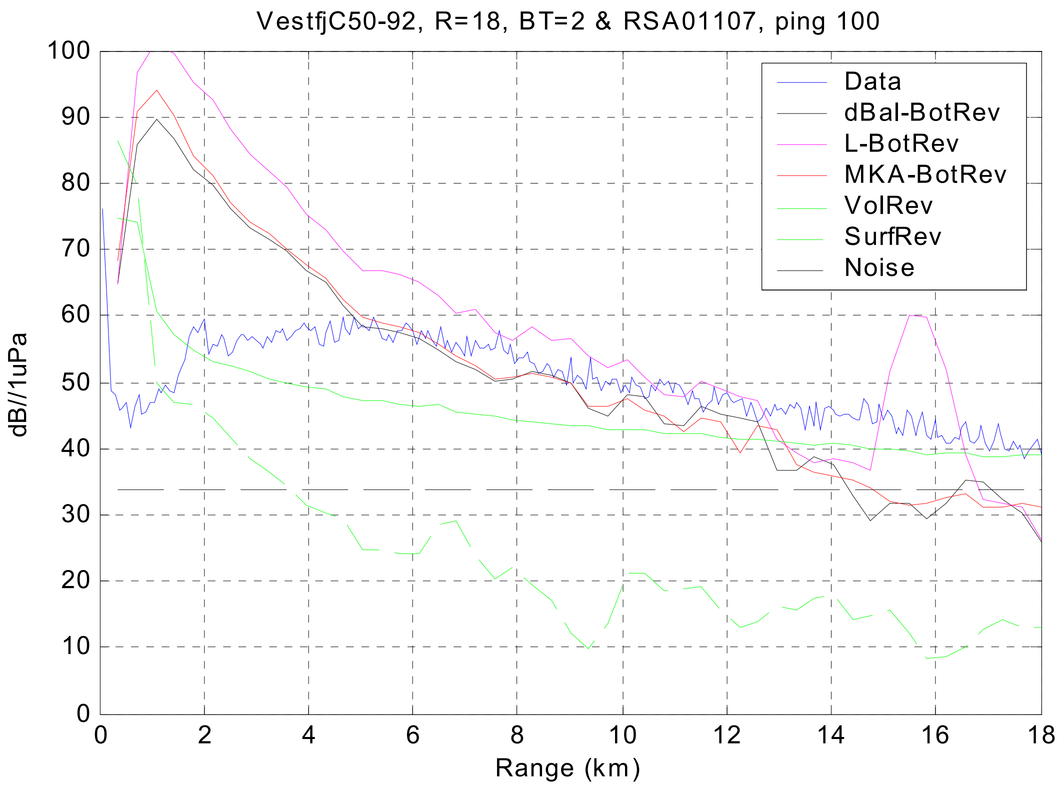

Figure A.19 Bottom reverberation variability is shown in sonar returns from 2 different pings from run 1, area A in Vestfjorden.

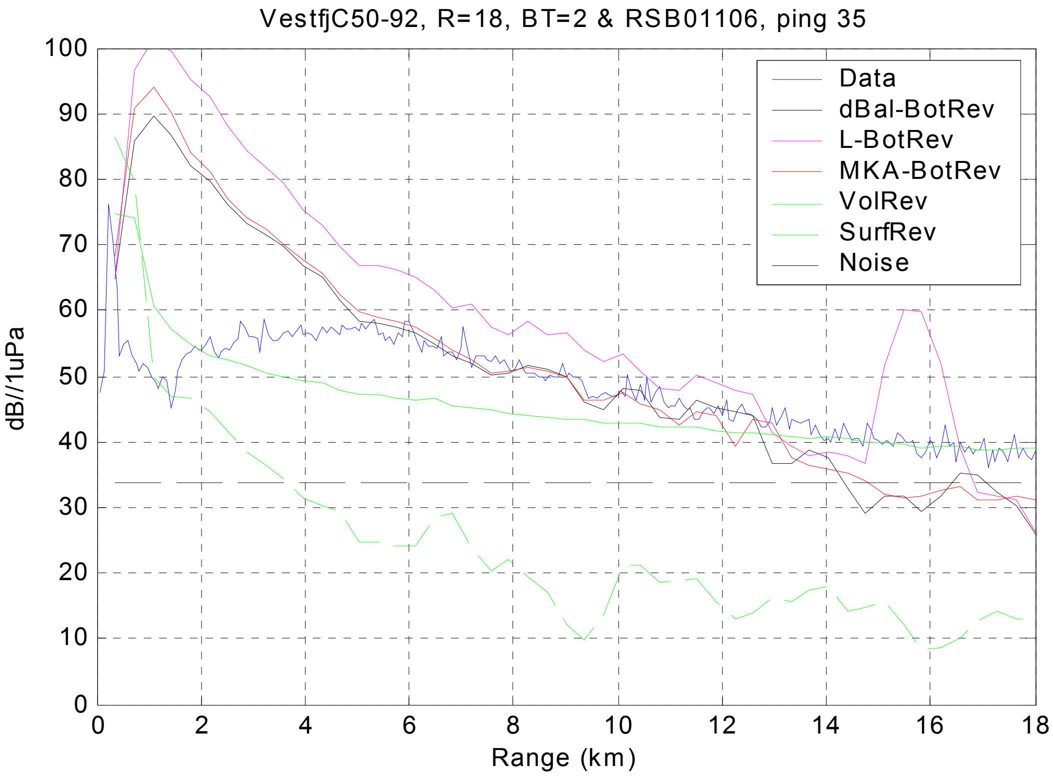

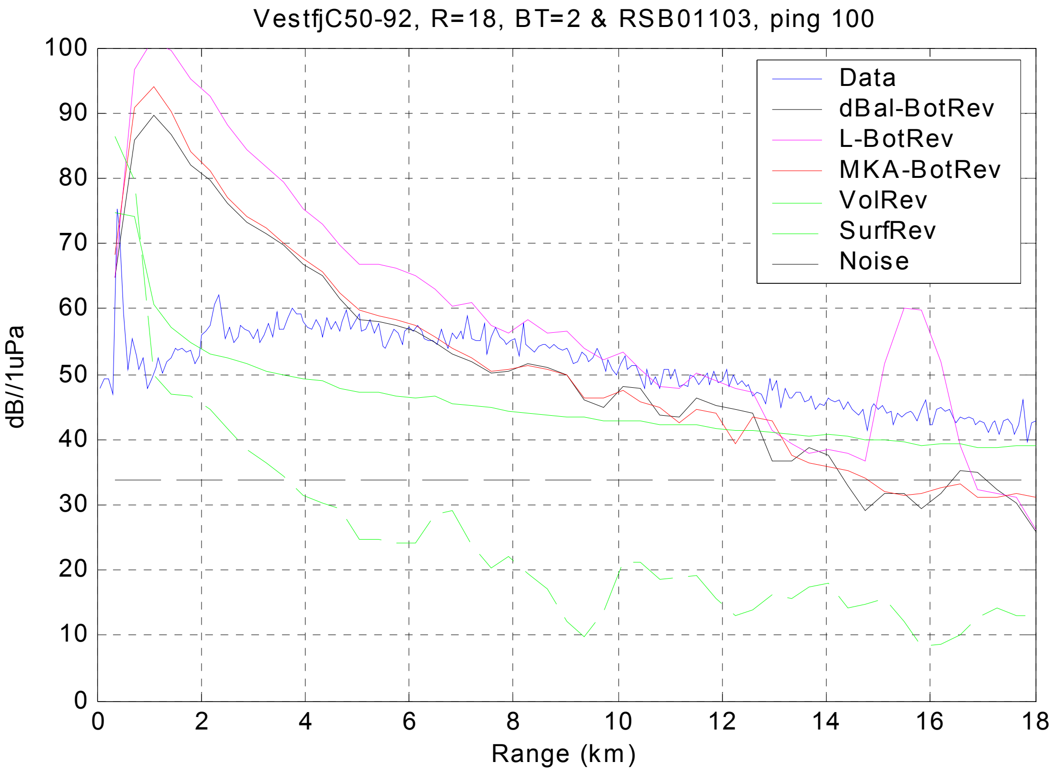

Figure A.20 Bottom reverberation variability is shown in sonar returns from 2 different pings from run 2, area B in Vestfjorden.

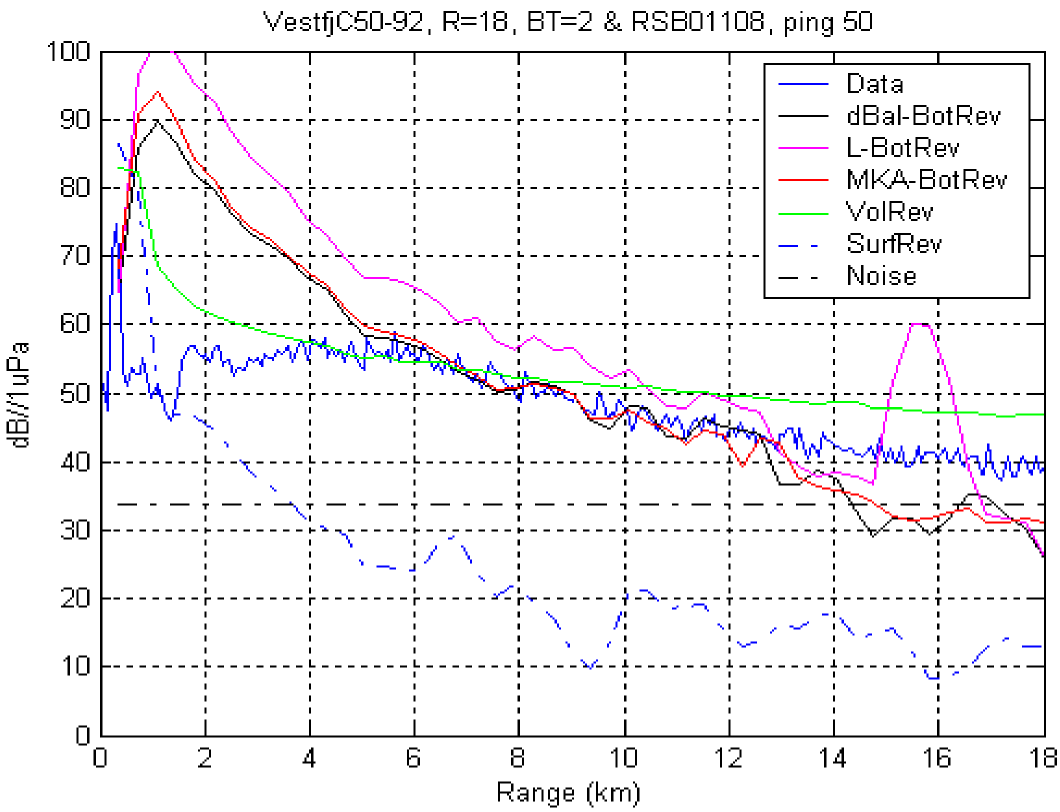

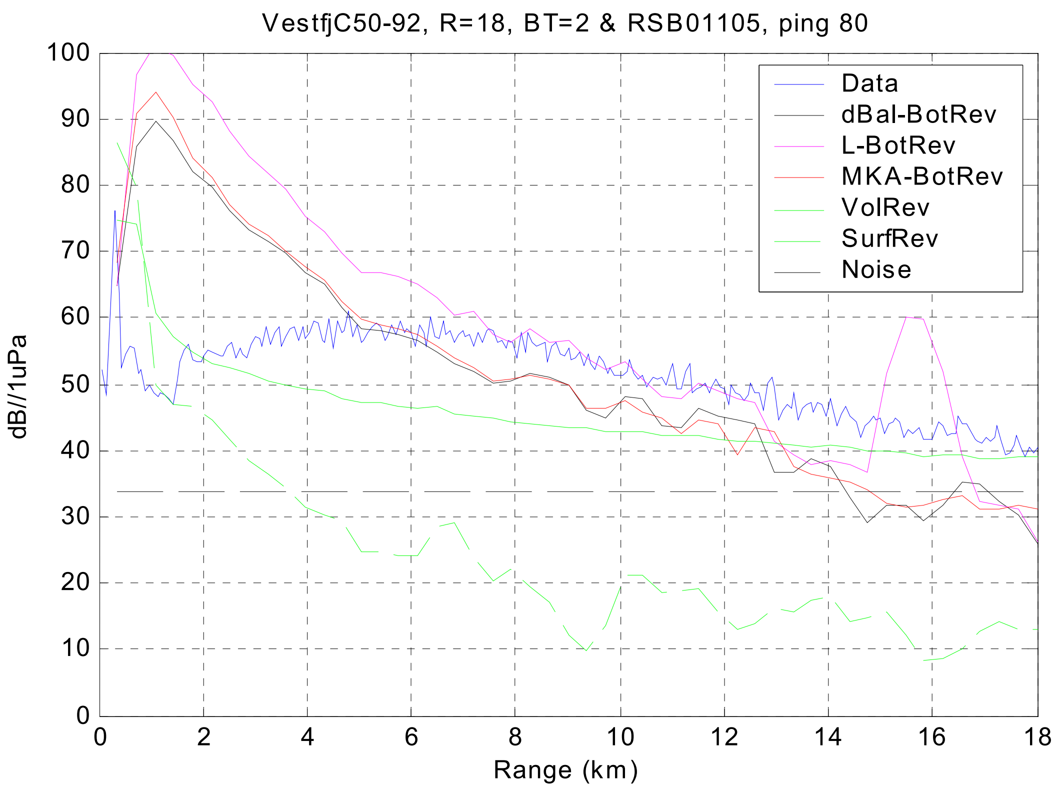

Figure A.21 Bottom reverberation variability is shown in sonar returns from 2 different pings from run 2, area B, Vestfjorden.

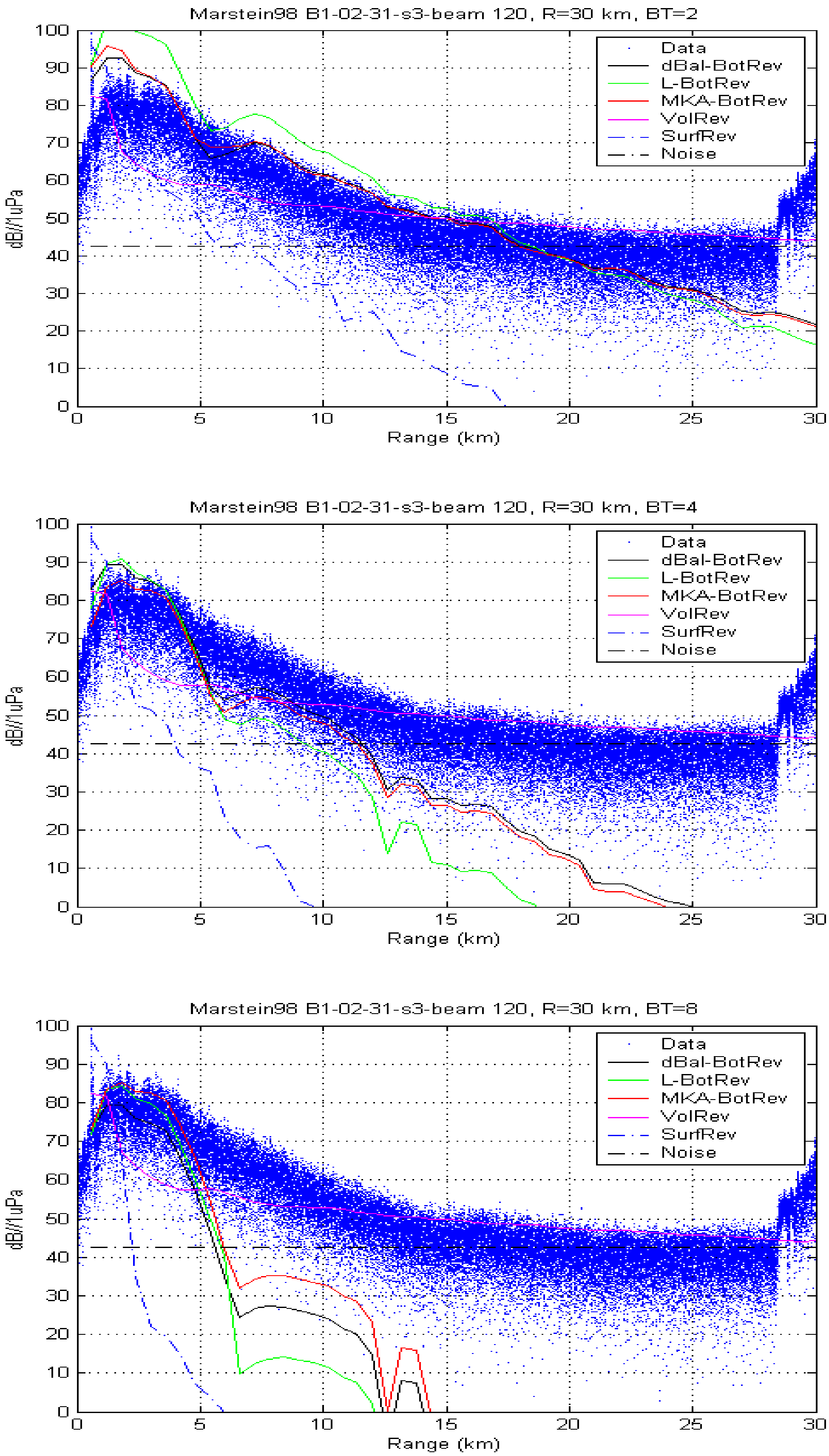

Figure A.22 CAPTAS sonar signals from Marstein98 compared with LYBIN simulations, test on bottom type. BT = 2 is obviously the right choice.

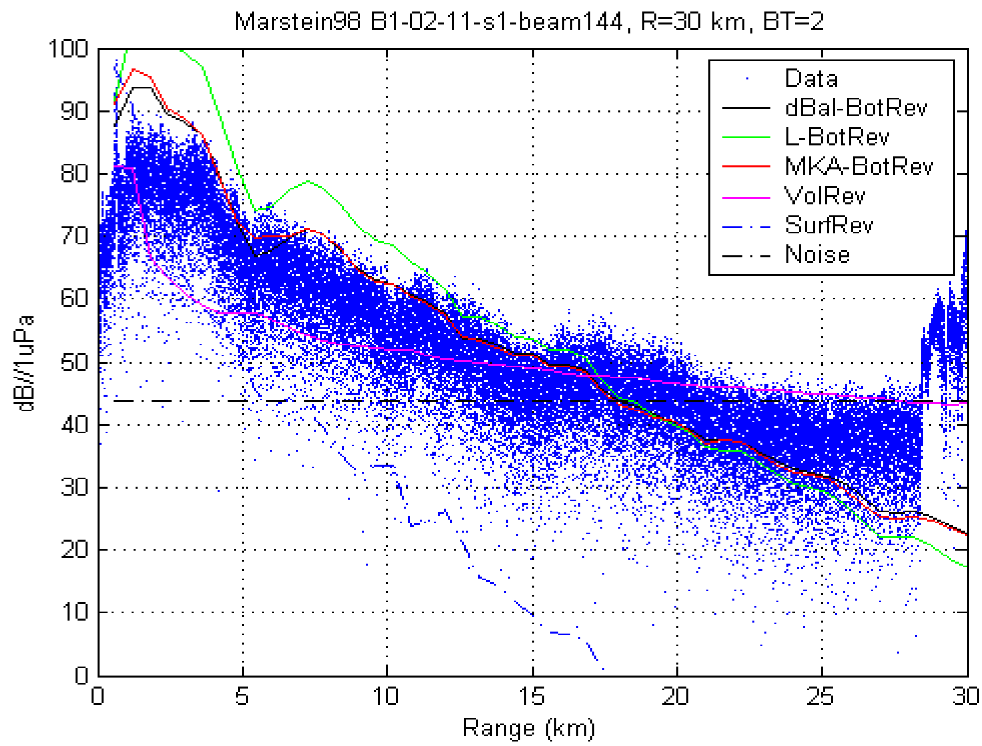

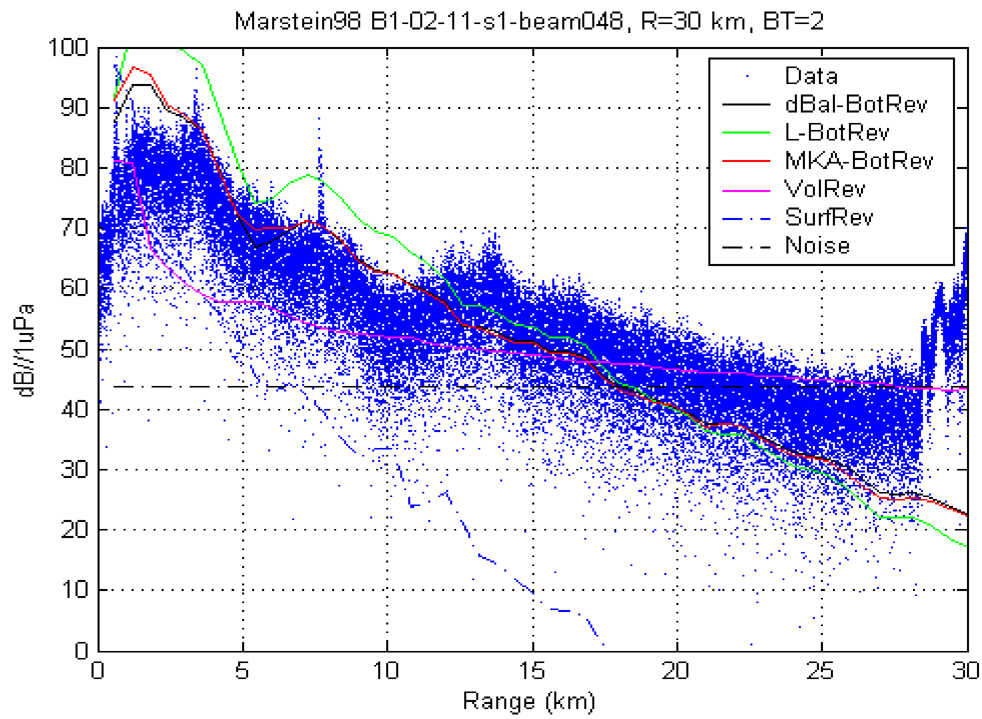

Figure A.23 CAPTAS sonar signals from Marstein98 compared with LYBIN simulations. Upper figure: Beam 144 pointing towards the open sea. Lower figure: Beam pointing towards land. (File B1_02_11_s1, 1. ping recorded from run DVB01)

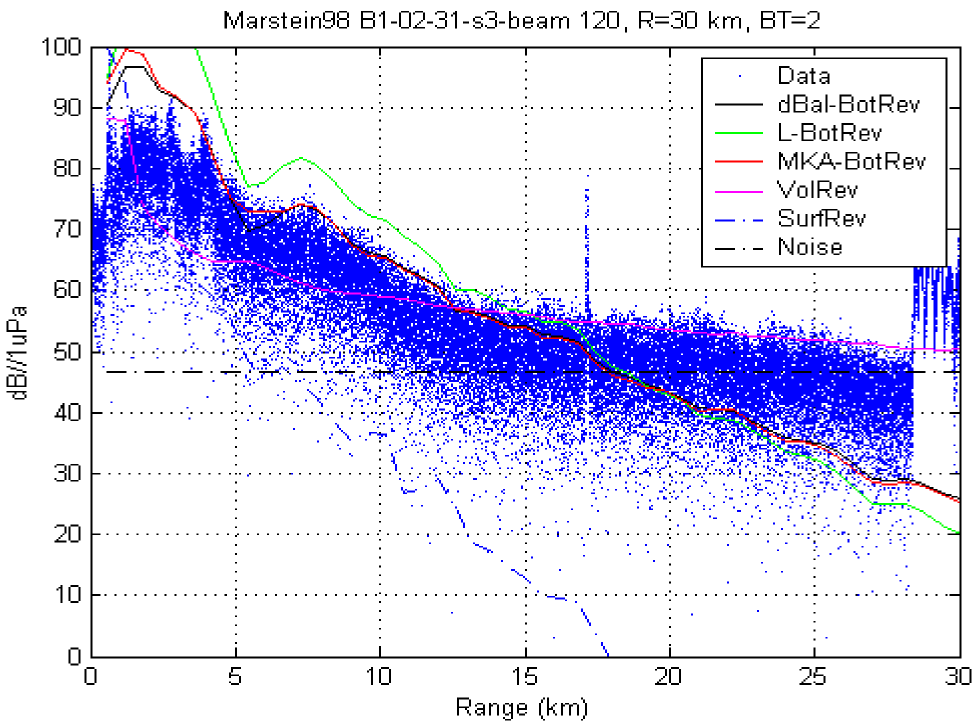

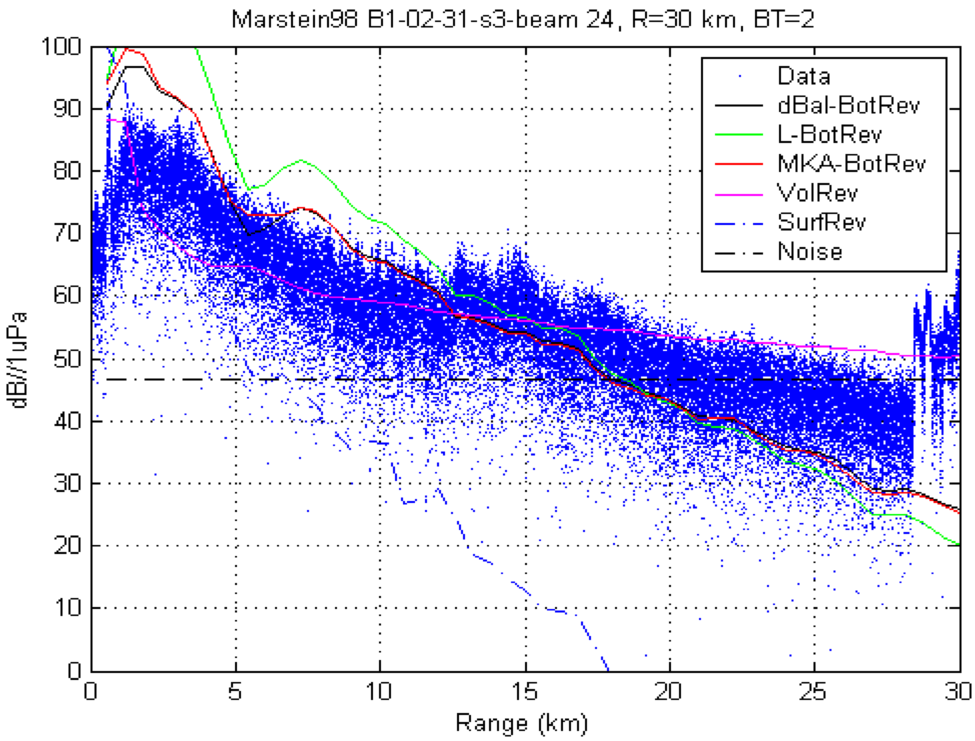

Figure A.24 CAPTAS sonar signals from Marstein98 compared with LYBIN simulations.
Upper figure: Beam 120 pointing towards the open sea.
Lower figure: Beam 24 pointing towards land
(File B1_02_31_s3, 27th ping recorded)

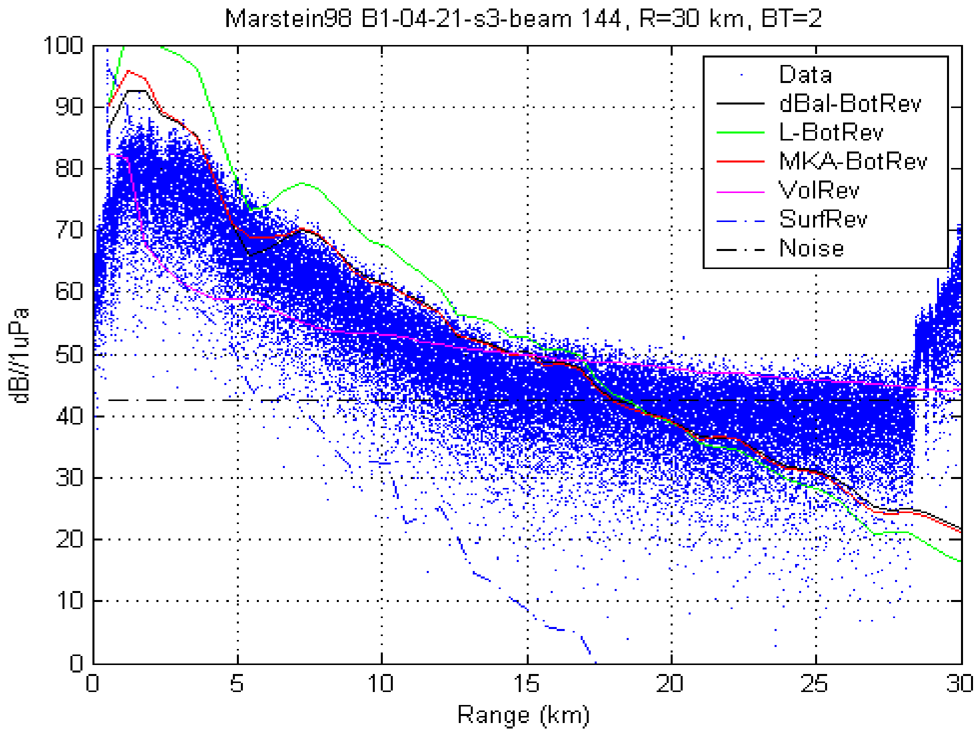

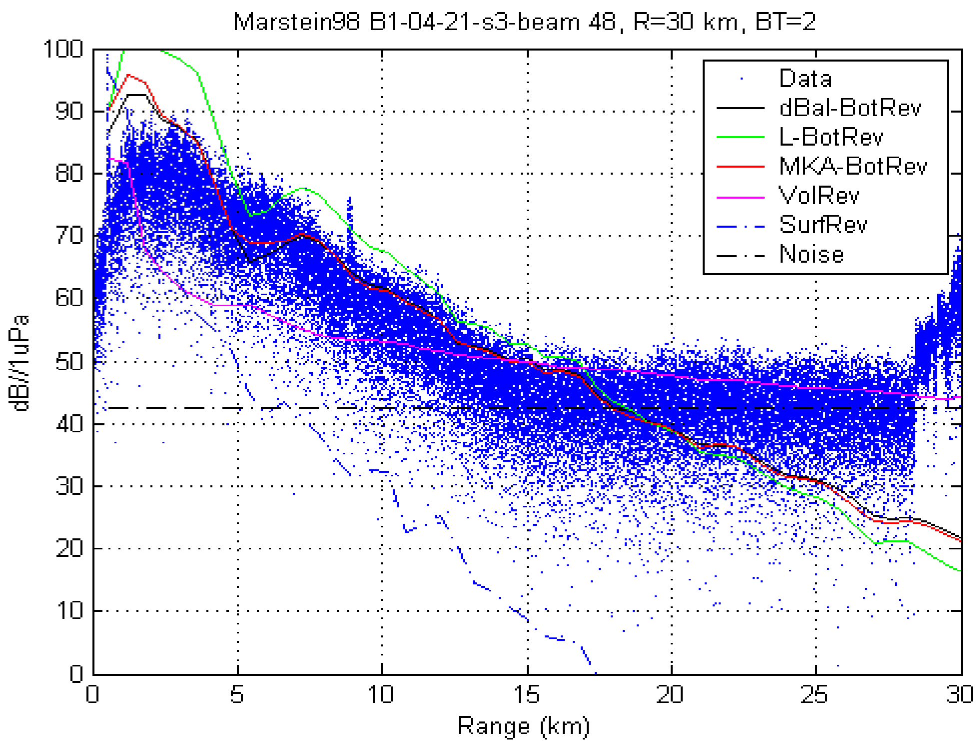

Figure A.25 CAPTAS sonar signals from Marstein98 compared with LYBIN simulations.
Upper figure: Beam 144 pointing towards open sea.
Lower figure: Beam 48 pointing towards land.
(File B1_04_21_s3, after 60 % of range (22 km))

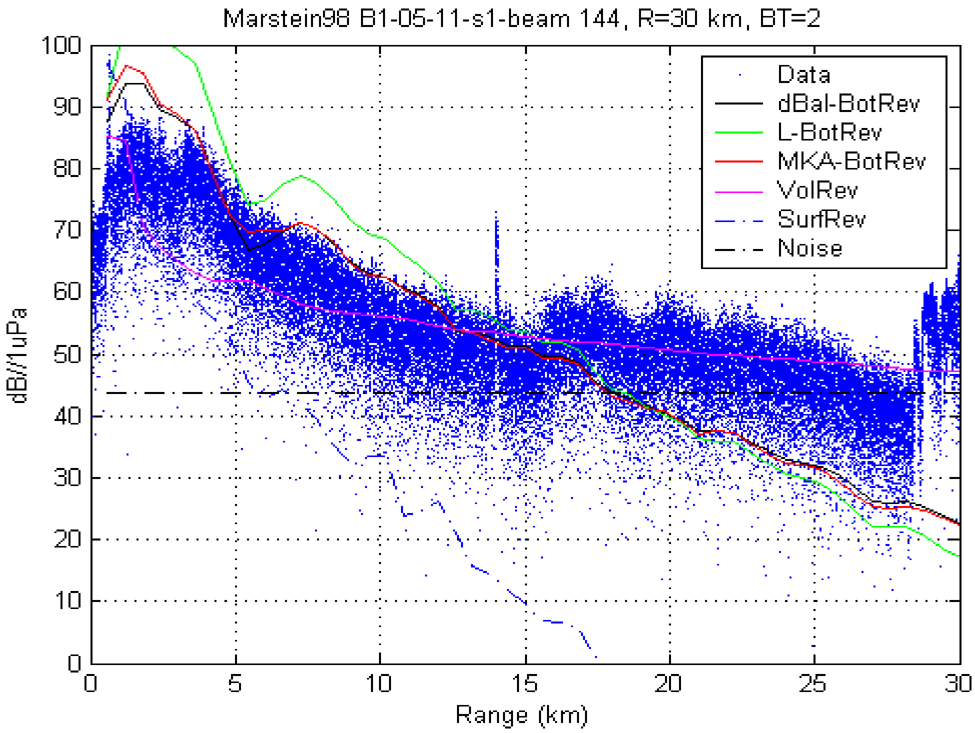

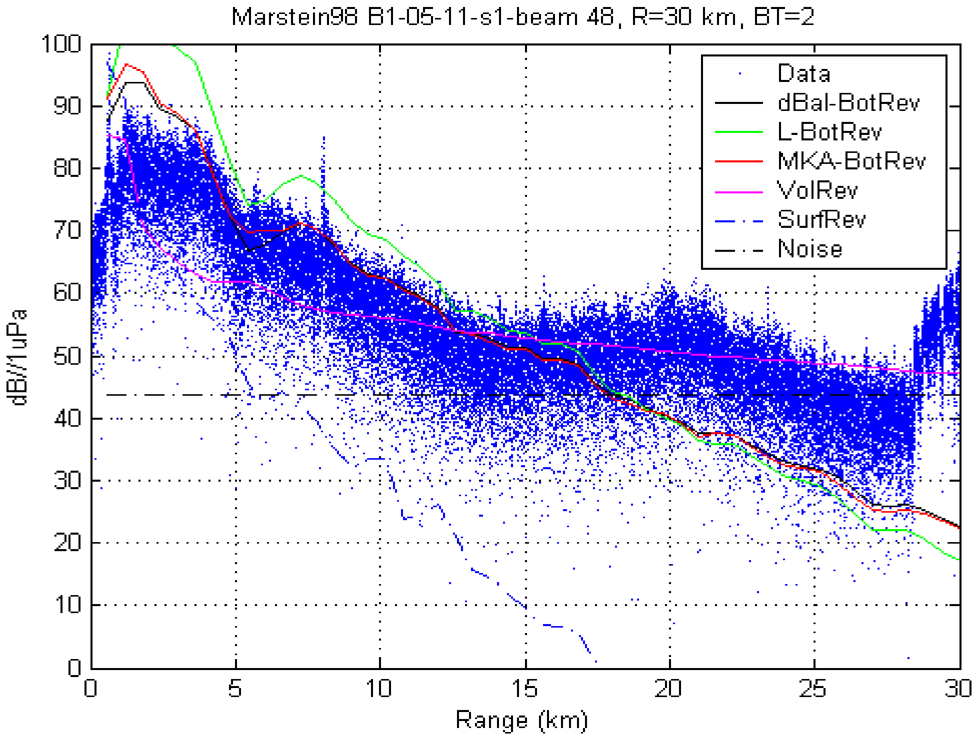

Figure A.26 CAPTAS sonar signals from Marstein98 compared with LYBIN simulations.
Upper figure: Beam 144 pointing towards open sea.
Lower figure: Beam 24 pointing towards land.
(File B1_05_11_s1, the 23 ping after B1_04_21_s3)

B LIST OF ABBREVIATIONS

BSC	Bottom Scattering Coefficient
CAPTAS	Combined Active/Passive Towed Array Sonar
delB	del Balzo (a BSC algorithm presented by del Balzo (3))
C50	CAPTAS sonar at 50 m depth
HMS	Hull Mounted Sonar
L	Lambert's rule
LYBIN	LYdBane og INtensitetsprogram, an acoustic model owned by NDLO
MKA	McKinney & Anderson (an empirical BSC algorithm invented by MK & A)
MRS2000	SPHERION HMS sonar for NF
NDLO	Norwegian Defence Logistics Organization
NF	New Frigates
POD	Probability Of Detection
REV	Reverbs, reverberation
S5	SPHERION sonar at 5 m depth
SPHERION	HMS for NF, type MRS2000
SVP	Sound Velocity Profile
THALES	French company, formerly TMS/Thomson
TML	Transmission Loss
TMS	Thomson/Marconi Systems
TUS	THALES Underwater Systems

Distribution list

FFIE **Dato:** 12. september 2002

RAPPORTTYPE (KRYSS AV)	RAPPORT NR.	REFERANSE	RAPPORTENS DATO
X RAPP ☐ NOTAT ☐ RR	2002/02367	FFIE/795/161.4	12. september 2002
RAPPORTENS BESKYTTEISESGRAD Unclassified		ANTAll EKS UTSTEDT 35	ANTAll SIDER 51
RAPPORTENS TITTEl BOTTOM REVERBERATION PREDICTIONS WITH THE ACOUSTIC MODEL LYBIN: A Comparison between three Bottom Backscattering Algorithms		FORFATTER(E) SEVALDSEN Erik	
FORDELING GODKJENT AV FORSKNINGSSJEF John-Mikal Størdal		FORDELING GODKJENT AV AVDELINGSSJEF: Johnny Bardal	

EKSTERN FORDELING

ANTALL	EKS NR	TIL
1		FLO/Sjø
1		v/Kommandør Per Erik Gøransson
1		v/Komkapt Christian Irgens
1		FO/SST
1		v/Okapt Steinar Willassen
1		SJOFF
1		v/Komkapt Halvard Flesland
1		KNM Tordenskjold
1		v/Okapt Per HL Engelsen
1		FO/E
1		v/Komkapt Per Erik Næss
1		FLO/Sjø T-S-SO
1		v/Kaptlt Harald Tholo
1		v/Senioring Svein Mjølsnes

INTERN FORDELING

ANTALL	EKS NR	TIL
14		FFI-Bibl
1		Adm direktør/stabssjef
1		FFIE
1		FFISYS
1		FFIBM
1		FFIN
1		Avdelingskontor FFIBM/Horten
1		Forfattereksemplar(er):
		ELEKTRONISK FORDELING:
		FFI-veven
		John-Mikal Størdal (JMS)
		Arne Cato Jenssen (ACJ)
		Stig Lødøen (SEL)
		Håkon Ljøgodt (JHL)
		Jahn Andreas Mæland (JAM)
		Frode Langset (FrL)
		Elin M. Dombestein (EMD)
		Harald Andås (HaA)
		Tor Knudsen (TKn)
		Elling Tveit (ETv)
		Jon Wegge (JWe)
		Trond Jenserud (TJe)
		Karl T. Hjelmervik (KTH)
		Erik Sevaldsen (ESe)

FFI-K1 Retningslinjer for fordeling og forsendelse er gitt i Oraklet, Bind I, Bestemmelser om publikasjoner for Forsvarets forskningsinstitutt, pkt 2 og 5. Benytt ny side om nødvendig.